

## Review

### Phenine design for nanocarbon molecules

By Koki IKEMOTO,\*<sup>1</sup> Toshiya M. FUKUNAGA\*<sup>1</sup> and Hiroyuki ISOBE\*<sup>1,†</sup>

(Edited by Keisuke SUZUKI, M.J.A.)

**Abstract:** With the name “phenine” given to 1,3,5-trisubstituted benzene for a fundamental trigonal planar unit to weave nanometer-sized networks, a series of curved nanocarbon molecules have been designed and synthesized. Since the  $6\pi$ -phenine units were amenable to modern biaryl coupling reactions mediated by transition metals, concise syntheses of  $>400\pi$ -nanocarbon molecules were readily achieved. In addition, the phenine design allowed for installing of heteroatoms and/or transition metals doped at specific positions of the large  $\pi$ -systems of the nanocarbon molecules. Fundamental tools were also developed to specify and describe the locations of defects/dopants, quantify pyramidalizations of trigonal panels and estimate molecular Gauss curvatures of the discrete surface. Unique features of phenine nanocarbons, such as stereoisomerism, entropy-driven molecular assembly and effects of dopants on electronic/magnetic characteristics, were revealed during the first half-decade of investigations.

**Keywords:** nanocarbons, phenine, organic synthesis, defects, curvature, molecular assembly

#### 1. Introduction

At the dawn of a structural theory leading to a valence bond theory in organic chemistry, Auguste Laurent coined the name “phène” for benzene and its derivatives.<sup>1),2)</sup> The term originated from the Greek words pheno/phainein (= to shine),<sup>‡</sup> referring to his discovery in illuminating gas by Faraday.<sup>3),4)</sup> Modern chemical terms such as “phenyl” and “phenylene” are, therefore, commemorating important contributions of Laurent in organic chemistry. With an emphasis on classification/nomenclature, Laurent summarized his systematic understanding of organic chemistry in a book, “*Chemical Method*”, which was finalized on his deathbed.<sup>5)</sup> In this book, we also find his legitimate concerns: “...when we reflect upon the absence of all system, all nomenclature, for the classification and denomination of this multitude of bodies, we demand with some anxiety, whether, in a few years’ time, it will be possible for us to direct

ourselves in the labyrinth of organic chemistry”. Almost 170 years later, we wonder if he would be delighted to find how today’s chemists explore the labyrinth by finding various paths on the firm basis of well-organized, modern organic chemistry.<sup>6)</sup>

Even after two centuries of development, introducing a conceptual term still seems to be valid for directing us to unique explorations in the field of organic chemistry.<sup>7)</sup> By coining the term “phenine” and using it as a light to illuminate our path, we have explored the labyrinth since 2017 (Fig. 1).<sup>§</sup> The labyrinth filled with large  $sp^2$ -carbon networks was explored by a series of nanocarbon “molecules” comprising networks of phenine, *i.e.*, 1,3,5-trisubstituted benzene, with the hope of obtaining a structural bases to understand the chemistry of nanocarbons. In this account, we wish to overview our first 5 years of study on “phenine nanocarbons”.

#### 2. Phenine design for nanocarbon molecules

Upon being connected in networks, the trigonal planar  $sp^2$ -carbon atoms naturally result in planar  $\pi$ -systems to afford two dimensional sheets of graphite/

\*<sup>1</sup> Department of Chemistry, The University of Tokyo, Tokyo, Japan.

† Correspondence should be addressed to: H. Isobe, Department of Chemistry, The University of Tokyo, Hongo 7-3-1, Bunkyo-ku, Tokyo 113-0033, Japan (e-mail: isobe@chem.s.u-tokyo.ac.jp).

‡ We wish to thank Prof. J.D. Tovar (Johns Hopkins University) for introducing us the original paper of Laurent.

§ The IUPAC preferred name for methine/phenine should be methanetriyl/benzene-1,3,5-triyl, although the term is rarely used. See Ref. 6.

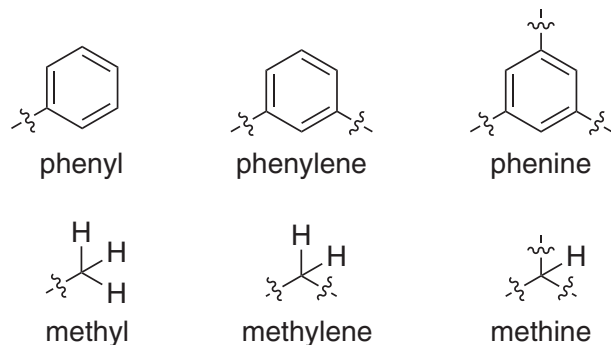


Fig. 1. Phenine design. The term “phenine” was coined by applying the “methyl/methylene/methine” nomenclature system to the phène series of “phenyl/phenylene”.

graphene. Introducing curvature to  $sp^2$ -carbon networks is hence challenging and intriguing, as demonstrated by the pioneering syntheses of  $[n]$ circulenes. The first example of a curved organic  $\pi$ -molecule was [5]circulene,<sup>8)–10)</sup> which was originally designated as corannulene.<sup>11),12),\*\*</sup> Later, interest in the synthesis/chemistry of curved  $\pi$ -molecules was dramatically ignited and fueled by the discoveries of nanocarbons, *i.e.*, fullerenes and carbon nanotubes,<sup>13),14)</sup> which recently led chemists to extensive studies of nanocarbons as “molecular entities”.<sup>15)</sup> The positive curvature of [5]circulene was inverted to negative curvature (see below for a detailed discussion on molecular curvature) when the polygon at the center was expanded to a heptagon in [7]circulene.<sup>16)</sup> The molecular shape was further contorted when the central polygon was changed to an octagon in [8]circulene.<sup>17),18)</sup> Nonetheless, there exists an intrinsic problem in the synthesis of curved organic  $\pi$ -molecules, which can be understood by examining the synthesis of the series of  $[n]$ circulenes. As shown in Fig. 2, each  $[n]$ circulene was independently elaborated by one-off, unique combinations of various reactions. Thus, although the structures are relevant, synthetic routes for each target need to be devised independently.

Although many curved organic  $\pi$ -molecules are currently being designed and synthesized,<sup>19),20)</sup> the syntheses unavoidably rely on one-off synthetic strategies. We thus envisaged that a common versatile strategy should accelerate the growth of this emerging field by expanding a structural library of nanocarbon molecules. Considering that one of the reasons for one-off syntheses was our inability to

handle an  $sp^2$ -carbon atom as an isolated unit, we came to the idea of using “phenine” as an alternative trigonal planar unit to design carbonaceous networks. This idea was also stimulated by the developments of modern biaryl coupling reactions.<sup>21)</sup> Robustness and versatility of the phenine design for the synthesis of unique nanocarbon molecules can be seen in various molecular structures that appear in this account. With four types of coupling reactions utilized thus far (Fig. 3),<sup>22)–27)</sup> various molecules, including one with  $>400\pi$  electrons and  $>7000$  Da, were synthesized. We will first describe fundamental hydrocarbon molecules (Fig. 2). Although the synthesis started from nanocarbon molecules that mimicked existing  $sp^2$  molecules, we immediately reached hypothetical yet-to-be-synthesized molecules.

### 3. Hydrocarbon phenine nanocarbons

**3.1. “Omphalos + periphery”: Phenine  $[n]$ circulenes.** The phenine design stemmed from our investigations of cycloarylenes. We took our first step in cycloarylene macrocycles by exploring of oligomeric macrocyclization via coupling for the synthesis. We found that Ni-mediated Yamamoto coupling was particularly suitable for macrocyclization, which led to the first synthesis of naphthylene macrocycles ( $[n]$ cyclo-2,7-naphthylenes;  $[n]$ CNAP)<sup>28)</sup> and to the revised synthesis of phenylene macrocycles ( $[n]$ cyclo-*meta*-phenylenes;  $[n]$ CMP)<sup>29)</sup> (Fig. 4). Another important step for the phenine design was site-selective borylation of  $[n]$ CMP by Ishiyama-Miyaura-Hartwig C-H borylation.<sup>30)–33)</sup> This highly efficient perborylation allowed us to use the  $[n]$ CMP macrocycles as an “omphalos” for the synthesis of phenine  $[n]$ circulenes.

Our phenine design of a series of  $[n]$ circulenes started in 2017. In brief, phenine  $[n]$ circulenes and their expanded derivatives were synthesized by one common strategy: periphery-forming units are introduced on a polygonal  $[n]$ CMP omphalos, and subsequent periphery-closing reactions complete the synthesis. The first example was phenine [5]circulene **1** (Fig. 2 and Fig. 5a).<sup>34)</sup> On a pentagonal omphalos of [5]CMP **9** ( $n = 5$ ), five terphenyl units (**10**) were introduced by Suzuki-Miyaura coupling, and the periphery was completed by closing hexagons of phenine by Ni-mediated Yamamoto coupling to afford phenine [5]circulene **1** ( $C_{160}H_{150}$ , 2073 Da,  $120\pi$  electrons). The overall yield of **1** having 25 biaryl bonds was 3% from 1,3-dibromobenzene. The X-ray crystallographic analysis unequivocally revealed the bowl-shaped structure of **1** (Fig. 5b).

\*\* The structure of [5]circulene led to a hypothetical proposal of  $C_{60}$ . See Refs. 11 and 12.

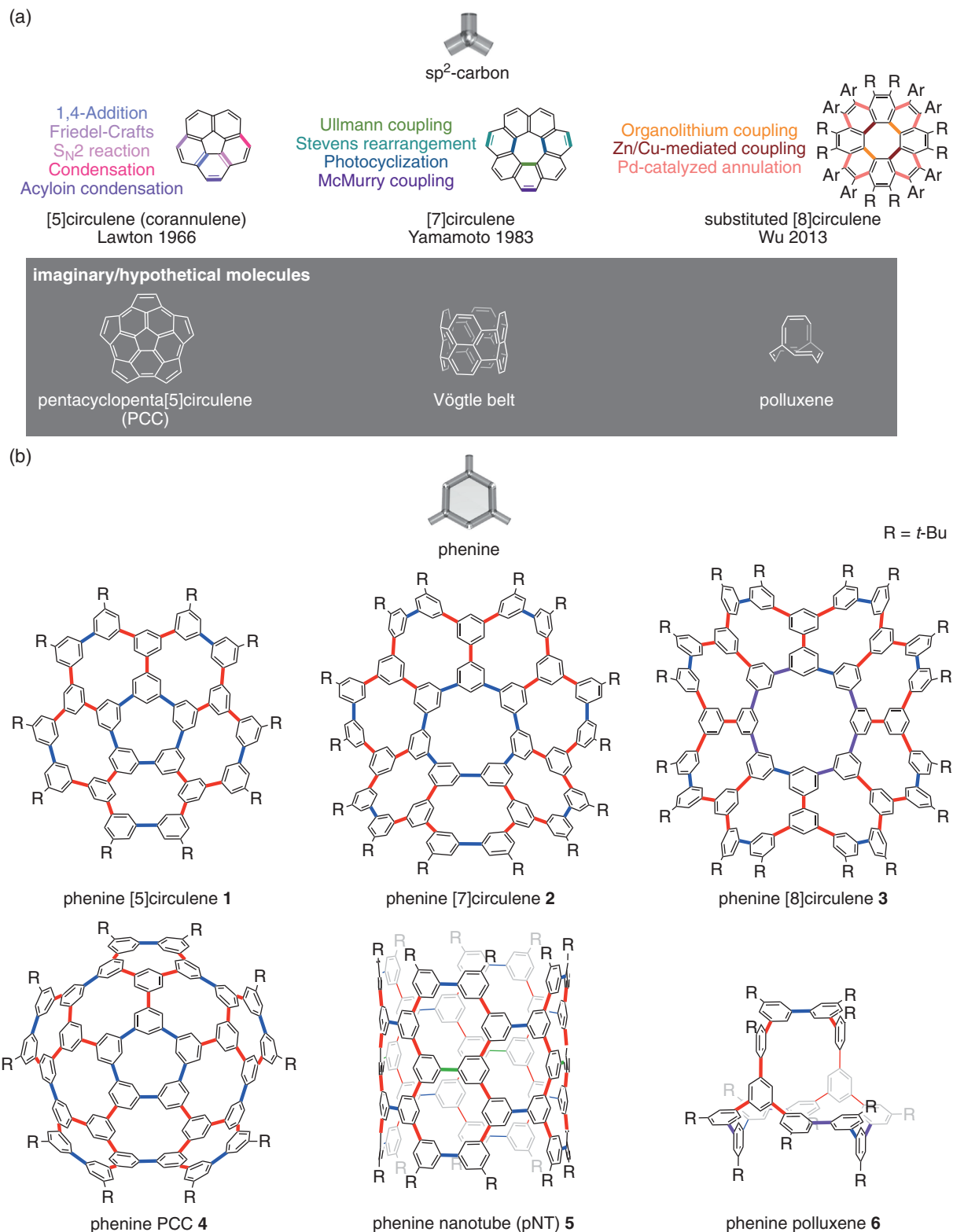


Fig. 2. Nanocarbon molecules designed by assembly of a planar trigonal unit. (a) Molecules with sp<sup>2</sup>-carbon atoms. (b) Molecules with phenine. See Fig. 3 for colors of biaryl bond-forming reactions.

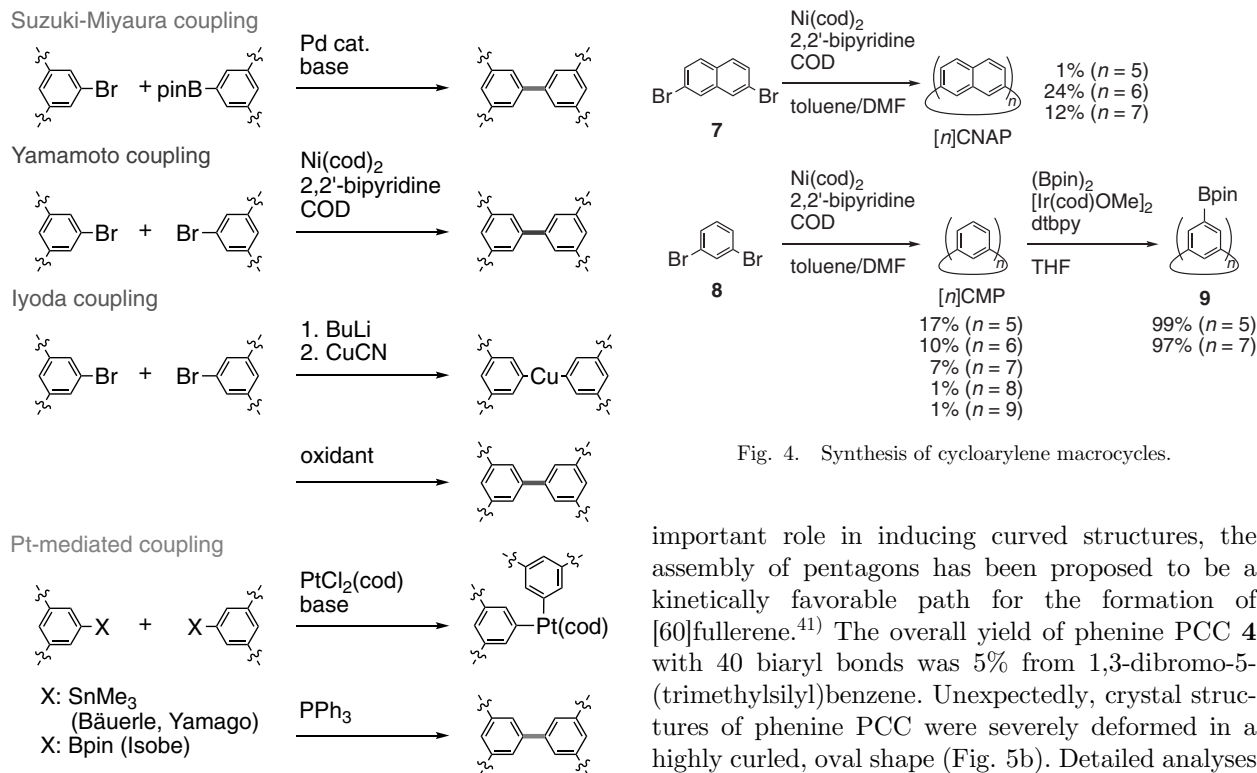


Fig. 3. (Color online) Biaryl coupling reactions used for phenine design (until 2022).

During synthetic studies toward [60]fullerene (C<sub>60</sub>),<sup>35,36</sup> a unique hydrocarbon, *i.e.*, pentacyclopenta[5]circulene (PCC; see Fig. 2), was conceived as an attractive candidate for synthetic intermediates.<sup>37–39</sup> Among various “C<sub>30</sub>” units from bisectonal retrosynthetic analysis, “cyclopenta-fused” [5]circulene, PCC, thus turned out to be the simplest bisection with the highest symmetry. Because of its difficult synthetic task, PCC still remains hypothetical, and an alternative synthetic route has been elaborated for the synthesis of [60]fullerene. We noticed that the phenine design can readily tolerate an extension of the network by enlarging periphery-forming units. Thus, in place of the “terphenyl” periphery-forming unit for **1**, we designed and introduced a “pentagon” periphery-forming unit and succeeded in the synthesis of phenine PCC (**4**) (Fig. 2).<sup>40</sup> Five pentagon units (**13**) were thus introduced to iodinated omphalos (**12**) by Suzuki-Miyaura coupling to afford a starfish-shaped precursor (**14**) (Fig. 5). Iododesilylation of **14** and subsequent periphery-closing reactions by Yamamoto coupling afforded phenine PCC **4** (C<sub>220</sub>H<sub>180</sub>, 2824 Da, 180π electrons). As pentagons play an

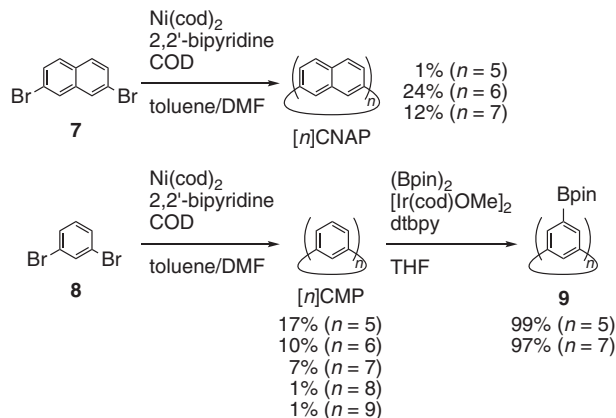


Fig. 4. Synthesis of cycloarylene macrocycles.

important role in inducing curved structures, the assembly of pentagons has been proposed to be a kinetically favorable path for the formation of [60]fullerene.<sup>41</sup> The overall yield of phenine PCC **4** with 40 biaryl bonds was 5% from 1,3-dibromo-5-(trimethylsilyl)benzene. Unexpectedly, crystal structures of phenine PCC were severely deformed in a highly curled, oval shape (Fig. 5b). Detailed analyses via the introduction of geometric measures revealed the origin of the structural deformation (see below).

By adopting heptagonal omphalos, the molecular shape was altered to a negatively curved saddle in the form of phenine [7]circulene (**2**) (Fig. 2).<sup>42</sup> The [7]CMP omphalos was obtained from our one-pot [n]CMP synthesis (Fig. 4), and an identical two-step transformation was adopted to synthesize phenine [7]circulene (**2**) (C<sub>224</sub>H<sub>210</sub>, 2902 Da, 168π electrons). Because the number of biaryl bonds increased, the overall yield of **2**, having 35 biaryl bonds, dropped to 0.1% from 1,3-dibromobenzene. A gigantic saddle shape of **2** was revealed by X-ray crystallography (Fig. 5b), which was further studied in detail including the molecular Gauss curvature (see below).

Although the phenine design from the [n]CMP omphalos was successful for [5]- and [7]circulenes, the lack of synthetic access to larger [n]CMP congeners hampered further explorations (see Fig. 4).<sup>43</sup>†† We thus developed a “4 + 4” dimerization route to synthesize [8]CMP.<sup>44</sup> Believing that this route could apply to other large [n]CMP congeners, we devised a unique optimization method by design-of-experiments (DoE) optimizations supplemented by ma-

†† For chemical terms, nonexperts may refer “IUPAC Gold Book (<https://goldbook.iupac.org>)”. We thank a reviewer for bringing our attention to this point. For example, see Ref. 43.

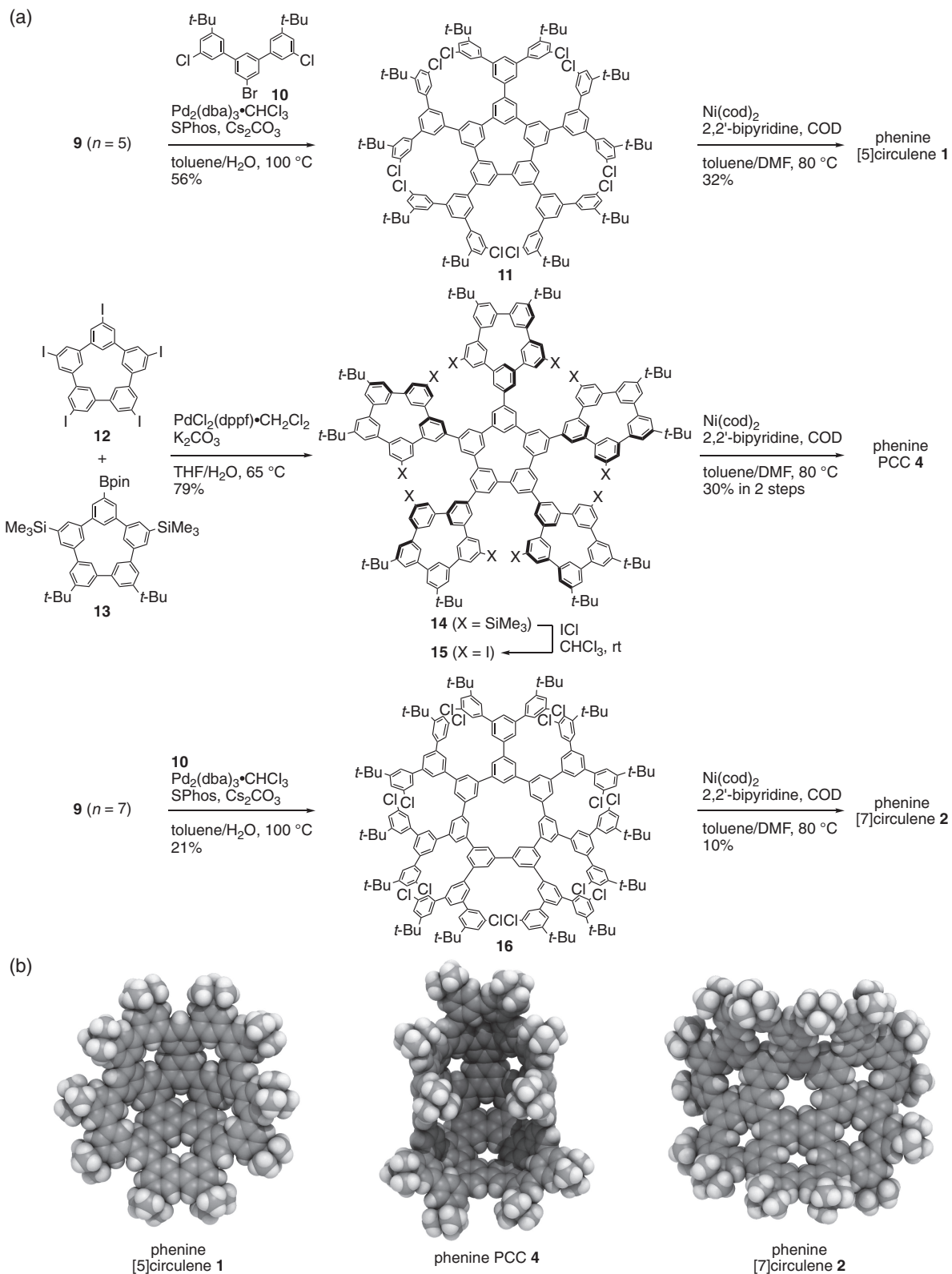


Fig. 5. Phenine [*n*]circulenes from “omphalos + periphery” synthesis. (a) Synthesis. (b) Space-filling models show crystal structures. One representative structure for each congener is shown.

chine-learning (ML) predictions. To synthesize dibrominated quaterphenyl (**17**), Iyoda coupling was adopted to preassemble three biaryl bonds in this precursor, which was subsequently subjected to a dimeric macrocyclization for the octagonal omphalos. As dimeric macrocyclization inevitably involves complicated competitions of multiple inter- and intramolecular reactions, the DoE + ML method was devised. In short, three major factors ( $M$  = equivalent of  $\text{Ni}(\text{cod})_2$ ,  $T$  = addition time of quaterphenyl,  $C$  = final concentration of quaterphenyl) were varied in three levels by filling the most efficient, DoE-directed combinations of 9 cells out of 81 cells of the synthetic parameter space. The data were then supplemented by ML predictions to obtain a heatmap for an overall view of the parameter space (Fig. 6). The synthesis of [8]CMP **18** was accomplished by using the optimum conditions derived from the DoE + ML method. While the oligomeric macrocyclization of dibromobenzene afforded **18** in a 1% yield (Fig. 4), the three-step synthesis recorded a 47% yield from dibromobenzene. The octagonal omphalos was then converted to phenine [8]circulene **3** ( $\text{C}_{256}\text{H}_{240}$ , 3317 Da,  $192\pi$  electrons) by three-step transformations via Ishiyama-Miyaura-Hartwig C-H borylation, Suzuki-Miyaura coupling and Yamamoto coupling. The overall yield of **3**, having 40 biaryl bonds, was 7% from 1,3-dibromobenzene, which was even larger than those of **1** and **2**. As shown in Fig. 6, the crystal structure was highly contorted in a saddle shape. To disclose the curvature quantitatively, we adopted the discrete surface theory of geometry and defined the molecular Gauss curvature in this molecule (see below).

### 3.2. "Hoop + edge": Phenine nanotubes.

Recent years have witnessed an ever-growing interest in the bottom-up synthesis of hoop-shaped nanocarbons because their radially oriented  $\pi$ -systems can serve as models to bring about an in-depth understanding of the unique properties of single-wall carbon nanotubes. Although a variety of such nanocarbon molecules, including [ $n$ ]cyclo-*para*-phenylenes ([ $n$ ]CPPs; so-called nano-hoops), have been synthesized to date,<sup>20,45–48</sup> the bottom-up synthesis of nanometer-sized architectures still poses a considerable challenge to chemists, particularly, in terms of the "lengths" of molecules.<sup>49</sup> We envisaged that our phenine design could readily construct nanometer-sized hoops and cylinders.

We first started with the synthesis of "phenine nano-hoops", *i.e.*, phenine [ $n$ ]CPP (Fig. 7a), via the assembly of phenine hexagons.<sup>50</sup> The phenine

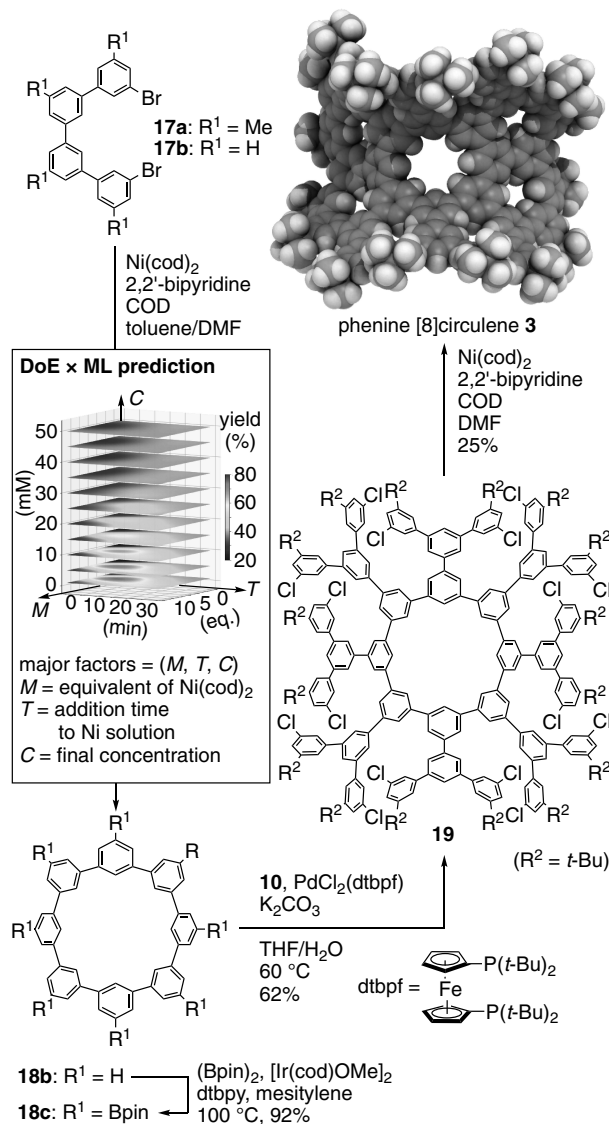


Fig. 6. (Color online) Synthesis of phenine [8]circulenes **3**. Design-of-experiments optimizations were supplemented by machine learning predictions to synthesize the octagonal omphalos. A space-filling model shows the crystal structure.

hexagon (**23**) was prepared by "3 + 3" cyclization with terphenyl (**22**), which was synthesized from dibromobenzene (**8**) via Miyaura borylation and Suzuki-Miyaura coupling. After installing boryl groups, the phenine hexagons were cyclized by Pt-mediated coupling to afford a series of oligomers. The yields were 3% for the trimer [phenine [3]CPP **25** ( $\text{C}_{156}\text{H}_{162}$ , 2037 Da,  $108\pi$  electrons)], 6% for the tetramer [phenine [4]CPP **26** ( $\text{C}_{208}\text{H}_{216}$ , 2716 Da,  $144\pi$  electrons)] and 3% for the pentamer [phenine [5]CPP **27** ( $\text{C}_{260}\text{H}_{270}$ , 3395 Da,  $180\pi$  electrons)].

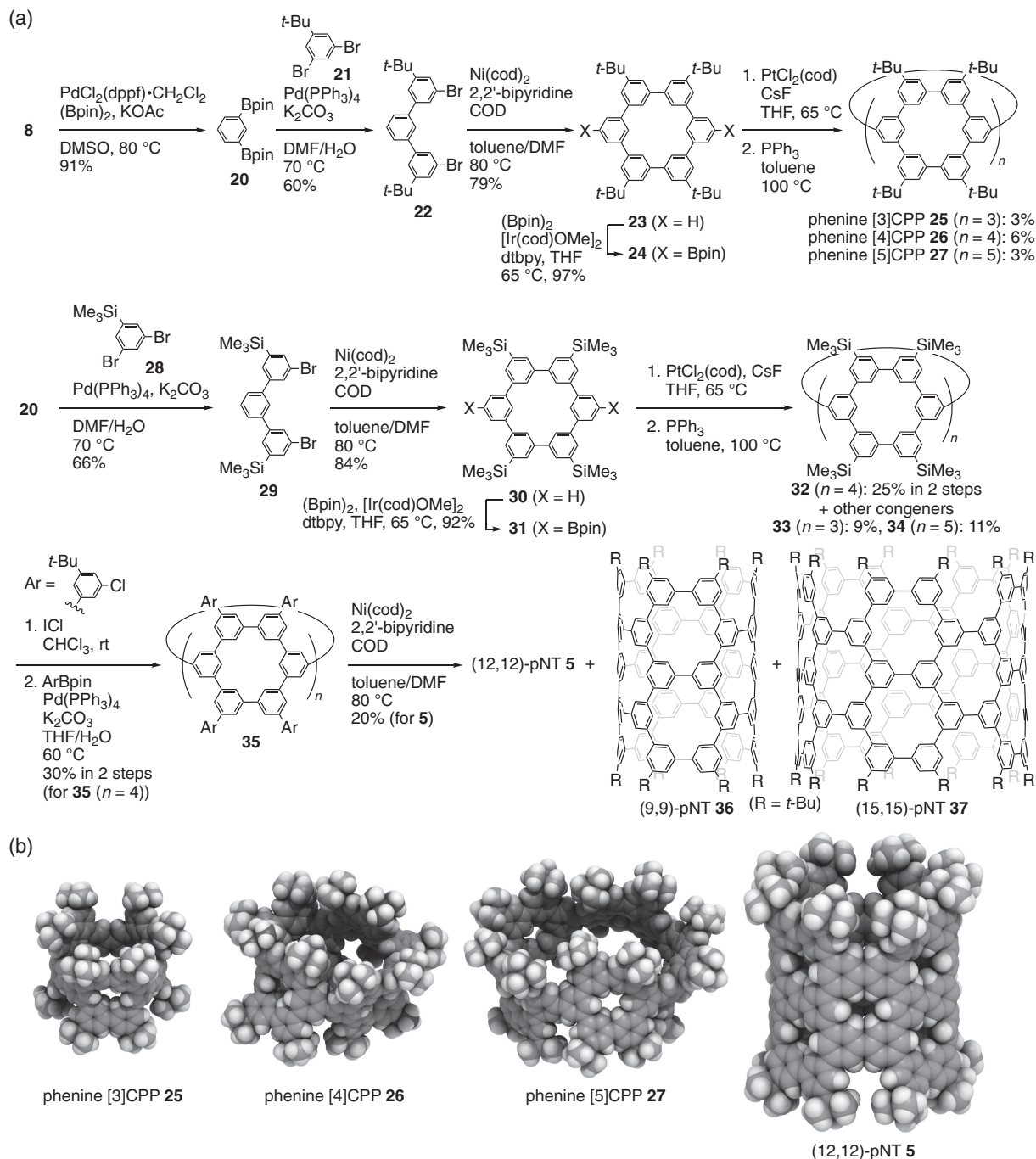


Fig. 7. “Hoop + edge” strategy. (a) Syntheses of pNTs (5, 36 and 37) and phenine CPP (25, 26 and 27). (b) Space-filling models show crystal structures.

Crystallographic analysis of phenine [ $n$ ]CPPs showed severely deformed shapes for larger congeners (26 and 27) (Fig. 7b) and, in combination with theoretical and spectroscopic analyses, revealed the occurrence of dynamic structural fluctuations in solution.

Phenine nanotubes (pNTs) were then synthesized.<sup>51</sup> The structures of pNT molecules are unique in that vacancy defects are embedded and distributed on the structures of carbon nanotubes (CNTs). The synthesis of pNT was completed by furnishing “edges”

on the phenine nanohoops (Fig. 7a). By replacing the *t*-Bu substituents of phenine [*n*]CPP (**25–27**), trimethylsilyl-functionalized phenine nanohoops (**32–34**) were prepared. On the edge of the nanohoops, 16 phenine units were installed via iododesilylation and Suzuki-Miyaura coupling, and the edges were stitched by Yamamoto coupling to furnish pNT molecule **5** (C<sub>304</sub>H<sub>264</sub>, 3917 Da, 240 $\pi$  electrons). In the 9-step transformation from 1,3-dibromobenzene, 52 biaryl bonds in pNT molecule **5** were formed with an overall yield of 0.7%, which corresponded to 91% bond-forming efficiency per biaryl bond. The length index ( $t_f$ ) of **5** was 7.0,<sup>49)</sup> which recorded the longest discrete nanotube molecule to date. Single-crystal X-ray crystallographic analysis revealed a nanometer-sized cylindrical structure with vacancy defects periodically introduced in the structure of the (12,12)-CNT molecule (Fig. 7b). Upon the kind requests of a reviewer of the original paper, we preliminarily completed the synthesis of narrowed and widened pNTs. Thus, minor nanohoop congeners **33** and **34** were isolated from the Pt-mediated cyclization and were subjected to the edge-closing process to afford (9,9)-pNT **36** (C<sub>228</sub>H<sub>198</sub>, 2938 Da, 180 $\pi$  electrons) and (15,15)-pNT **37** (C<sub>380</sub>H<sub>330</sub>, 4897 Da, 300 $\pi$  electrons).

### 3.3. “Transannulation”: Phenine polluxenes.

Phenine nanocarbons from a pentagon, hexagon, heptagon and octagon have been shown in the examples described above. How about larger polygons? Are there any unique features? With a decagon, we found a molecule that could answer an interesting question originating from mathematics.<sup>52)</sup> On July 11, 2009, Professor Motoko Kotani, a mathematician, asked the following question: “*Can you synthesize a decagonal network of sp<sup>2</sup>-carbon atoms?*” The question referred to a hypothetical network proposed by Sunada in 2008.<sup>53)</sup> By scrutinizing the structures of diamond, Sunada found “strong isotropy” and “maximal symmetry” as important features that could define the beauty of the network. Furthermore, he noticed that these two key features could also be maintained, even when the four-hand tetravalent vertices of diamond were replaced by three-hand, trivalent vertices by fulfilling structural requirements: the trivalent vertices need to be assembled in an array of decagonal cages. The network designated as the  $K_4$  lattice was mathematically rediscovered and was indeed visited many times with different names.<sup>‡‡</sup> The network has

even been examined as a hypothetical carbonaceous network of sp<sup>2</sup>-carbon atoms.<sup>54)</sup> However, the network forces two adjacent vertices to have nonplanar, twisted orientations, which severely lowers its stability and jeopardizes its existence.<sup>55),56)</sup>

During our explorations of the phenine design, the question of Professor Kotani somehow returned to us, which led us to the synthesis of “phenine polluxene”. In our work, the imaginary network of the carbonaceous  $K_4$  lattice and its minimum cage were named pollux and polluxene, respectively, considering that this entity was also referred to as a diamond twin, and the synthesis of a phenine version of polluxene was accomplished.

The unique network of polluxene comprises 14 vertices that form triply fused decagons. For the synthesis of phenine polluxene (**6**), a “transannulation route” was developed (Fig. 8). The first decagonal macrocycle (**41**) was synthesized by “5 + 5” cyclization of quinquephenyl (**40**) that was prepared from 1,3-dibromo-5-*t*-butylbenzene (**21**) via Iyoda coupling, Suzuki-Miyaura coupling and Ishiyama-Miyaura-Hartwig C-H borylation. The decagonal ring was then furnished with two biphenyl units by Suzuki-Miyaura coupling, and the bascule biphenyl bridges were finally closed by Yamamoto coupling to afford phenine polluxene **6** (C<sub>132</sub>H<sub>150</sub>, 1735 Da, 84 $\pi$  electrons). In the 6-step synthesis from **21**, 14 biaryl bonds were formed with an overall yield of 3.6%, which corresponded to 80% bond-forming efficiency per biaryl bond. Single-crystal X-ray crystallographic analysis revealed a  $D_3$ -cage structure composed of triply fused decagons of phenine vertices.

An interesting feature of the pollux network is its unique stereoisomerism: unlike a diamond network, “nonsuperposability” coexists with “strong isotropy” and “maximal symmetry” in this network. In the crystal, two enantiomeric conformers were indeed found and were designated the (*P*)- and (*M*)-forms, which described the helicity of three bridges around the  $C_3$  main axis of the molecule. In phenine polluxene, there are 15 biaryl bonds, and biaryl atropisomerism can give rise to 5600 nonredundant isomers (see below). However, because of flexible biaryl linkages, stereochemical rigidity, *i.e.*, a necessary condition for chirality, did not exist with **6**. Chiral polluxene was then realized by installing an *ortho*-dimethylated linkage. The “transannulation route” was versatile enough to tolerate concise installation of substituents, and two versions of chiral phenine polluxene were synthesized. A congener (**44**) with two *ortho*-methyl groups and two *meta*-me-

‡‡ See Supporting Information of Ref. 52 for further details.

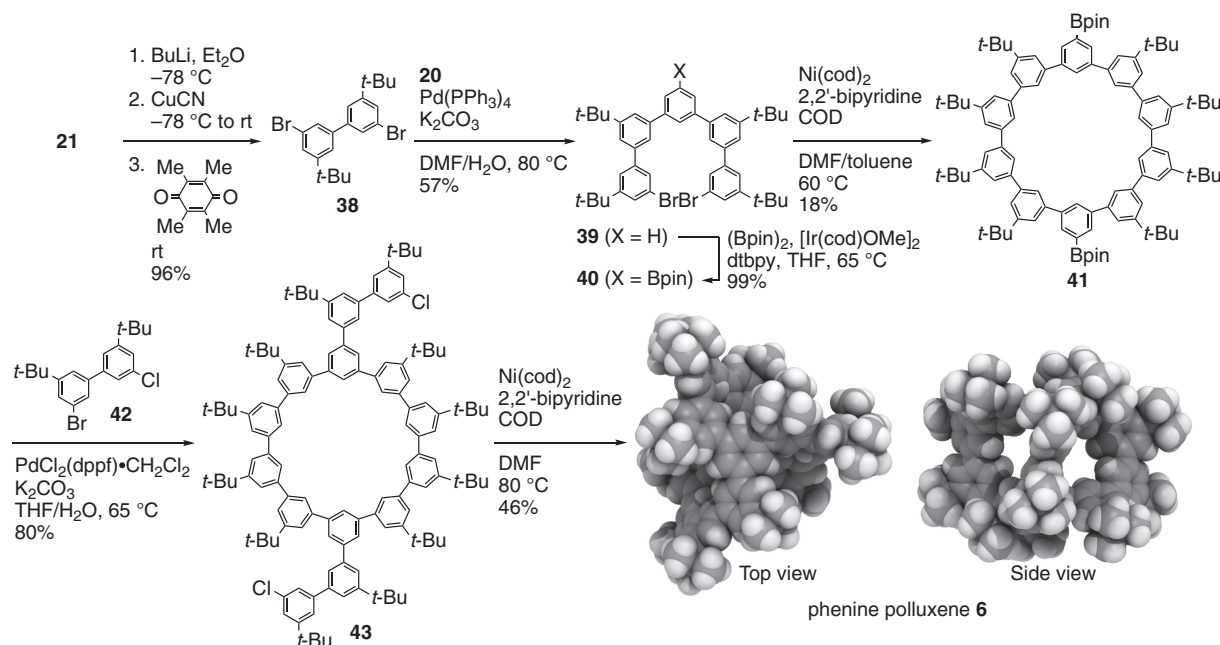


Fig. 8. Synthesis of phenine polluxene **6**. Space-filling models show crystal structures of the (*P*)-enantiomer as a representative example.

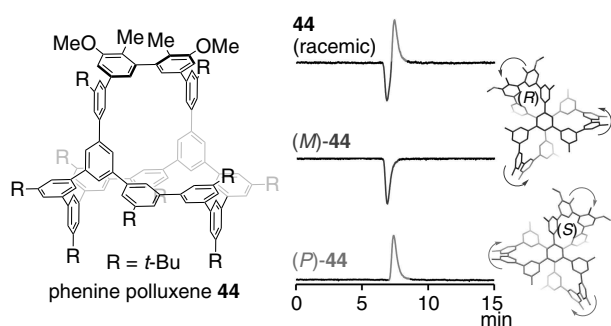


Fig. 9. (Color online) Chiral phenine polluxene **44**. Optical resolution was achieved by high-performance liquid chromatography (HPLC) with chiral columns.

thoxy groups installed on one bridge was suitable for optical resolution with a chiral column (Fig. 9). The optical resolution afforded (*P*)- and (*M*)-forms of phenine polluxene **44** with stable chirality, which represents an important feature of the chiral three-dimensional network of phenine pollux.

#### 4. Doped phenine nanocarbons

##### 4.1. Nitrogen-doped phenine nanotubes.

The versatility of the phenine design has also been demonstrated in its application of heteroatom doping. While doped nanocarbons are attracting much attention in materials science, with nitrogen-doped carbon nanotubes being the first exam-

ples,<sup>57–59</sup> in-depth, atomic-level understandings of dopant effects have been severely hampered by the lack of doped nanocarbon “molecules”. The phenine design readily allows for the replacement of phenine with doped congeners, and 2,4,6-trisubstituted pyridine was adopted for the first demonstration. Thus, following the synthetic route of pNT, N-doped phenine nanotubes (NpNTs) were synthesized (Fig. 10a).<sup>60</sup> Starting from 1-bromo-3-chlorobenzene **45**, we prepared N-doped [6]CMP **51** in 5 steps. The nitrogen dopants in **51** were compatible in the subsequent transformations of Pt-mediated macrocyclization, iododesilylation, Suzuki-Miyaura coupling and edge closure by Yamamoto coupling to afford NpNT **55** (C<sub>296</sub>H<sub>256</sub>N<sub>8</sub>, 3925 Da, 240π + 16n electrons). From 1-bromo-3-chlorobenzene **45**, 52 biaryl bonds in NpNT **55** were formed in 10 steps with an overall yield of 1.4% to embed 8 pyridinic nitrogen dopants with the structure. Single-crystal X-ray crystallographic analysis confirmed the N-doped cylindrical structure, and crystallographic charge density analyses revealed lone-pair electrons on the nitrogen dopants (Fig. 10b). Structural descriptions and electronic properties of NpNTs are described below.

In principle, three distinct atomic types of N-dopants, *i.e.*, pyridinic, pyrrolic and graphitic nitrogen atoms, should be possible and should dramatically alter the dopant effects. However, such atomic-

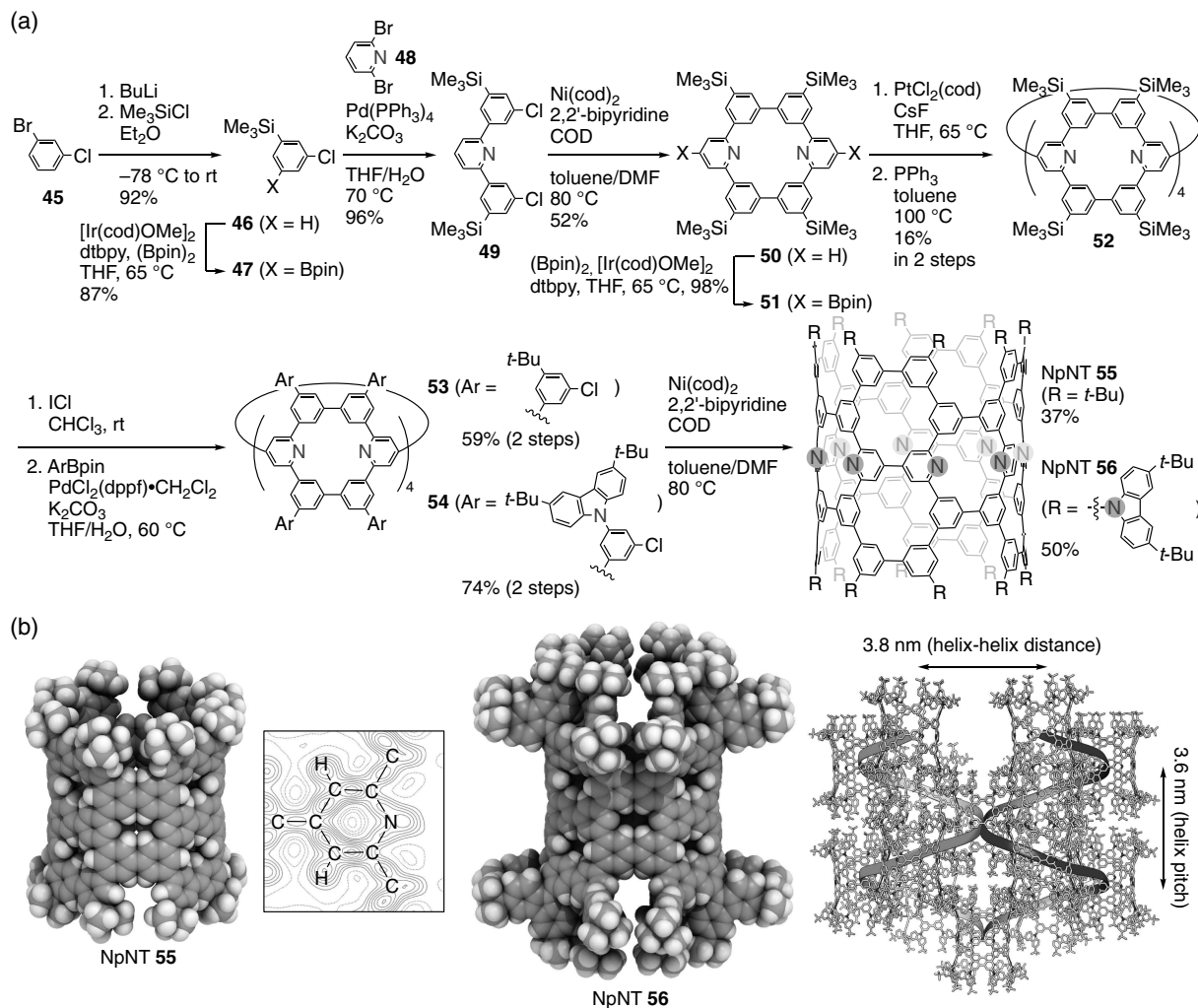


Fig. 10. (Color online) Nitrogen-doped pNT. (a) Synthesis of NpNTs **55** and **56**. (b) Space-filling models show crystal structures. For NpNT **55**, an experimental deformation map of the lone-pair electrons is shown. For NpNT **56**, a packing structure of a unique helical assembly is shown.

level structures could not be defined with nano-carbons (chemical species), which resulted in a controversial discussion on the role of the N-dopants.<sup>61)–63)</sup> By introducing pyrrolic nitrogen atoms at the edge of the NpNT cylinder, we succeeded in synthesizing NpNT **56**, which has pyrrolic and pyridinic nitrogen atoms doped at specific positions.<sup>64)</sup> The synthesis of second-generation NpNT **56** was straightforward with the phenine design (Fig. 10a). In place of the *t*-butyl group, carbazolyl-functionalized phenine units were installed at the edge of hoop **54**, and NpNT **56** ( $C_{552}H_{496}N_{24}$ , 7466 Da,  $464\pi + 16n$  electrons) was obtained by the edge-closure reaction utilizing Yamamoto coupling. This molecule provided an

interesting test case for examining the electronic contributions of nitrogen dopants (see below). The molecular structure of NpNT **56** was unequivocally confirmed by single-crystal X-ray crystallographic analysis (Fig. 10b). To the best of our knowledge, this molecule represents the largest synthetic molecule with C, H and N elements to be identified by X-ray crystallographic analysis. The analysis revealed that 16 carbazolyl groups at the rim of NpNT **56** were oriented in a cross-shaped fashion with respect to the cylindrical core. The carbazole rims render the cylindrical molecules aligned in a helical array. Right-handed and left-handed helices with a pitch of 3.6 nm coexisted in the crystal to form a racemic crystal.

#### 4.2. N- and M-doped phenine nanocarbons.

The nitrogen dopant was found to be effective in promoting oligomeric macrocyclization in a metal-templated manner. Thus, a unique synthetic method, named “metal-templated oligomeric macrocyclization via coupling (MOMC)”, was developed (Fig. 11a).<sup>65</sup> Several years after our initial, unsuccessful attempts at MOMC,<sup>66</sup> we found that dramatic change could be brought about simply by using an excess amount of Ni(cod)<sub>2</sub>. Thus, when dihalogenated pyridine **57** was subjected to Yamamoto coupling by using 10 equivalents of a Ni complex, one compound was selectively obtained in a 53% yield. Unexpectedly, the compound retained Ni after workups and chromatography and was a paramagnetic complex. Single-crystal X-ray crystallographic analysis revealed a rare pentagonal bipyramidal Ni(II) center located in a cyclic oligopyridyl with 5 panels (COPy-5) (NiCl<sub>2</sub>•**58**; Fig. 11b). The MOMC was concise enough for a scale-up synthesis and enabled the preparation of 1.77 g of NiCl<sub>2</sub>•**58** (57% yield) in one batch. Unique paramagnetic characteristics in nuclear magnetic resonance (NMR) spectra and detailed structural evaluations are described below.

The MOMC method was concise and amenable to  $\pi$ -extension (Fig. 11a). Thus, the presence of a terphenyl substituent on dihalogenated pyridine did not affect the reaction, and MOMC of **59** afforded NiCl<sub>2</sub>•**60** in a 46% yield. Subsequent iododesilylation and periphery-closing reactions proceeded in the presence of the Ni center, and N/Ni-doped, bowl-shaped phenine nanocarbons, NiCl<sub>2</sub>•**62** (C<sub>155</sub>H<sub>145</sub>N<sub>5</sub>NiCl<sub>2</sub>, 2207 Da, 120 $\pi$  + 10n + 8d electrons) were synthesized. Single-crystal X-ray diffraction analysis of NiCl<sub>2</sub>•**62** revealed a contorted, bowl-shaped structure with a pentagonal bipyramidal Ni center located at the center of a 3-nm bowl (Fig. 11b).

### 5. Methods for structural analyses/descriptions

**5.1. Coordinate nomenclature: Defining locations of defects in nanotubes.** For any chemistry discussions based on molecular structures, specification and designation of structures are undoubtedly important. For instance, *ortho*, *meta* and *para* prefixes are essential for any discussion/comparisons of disubstituted benzene isomers, which deepens our understanding of molecular science via structure-property relationship studies.<sup>67)–69)</sup> With heteroatoms doped at the specific positions of NpNT nanotubes, various possible “isomers” emerge, and designations/specifications of the structures are

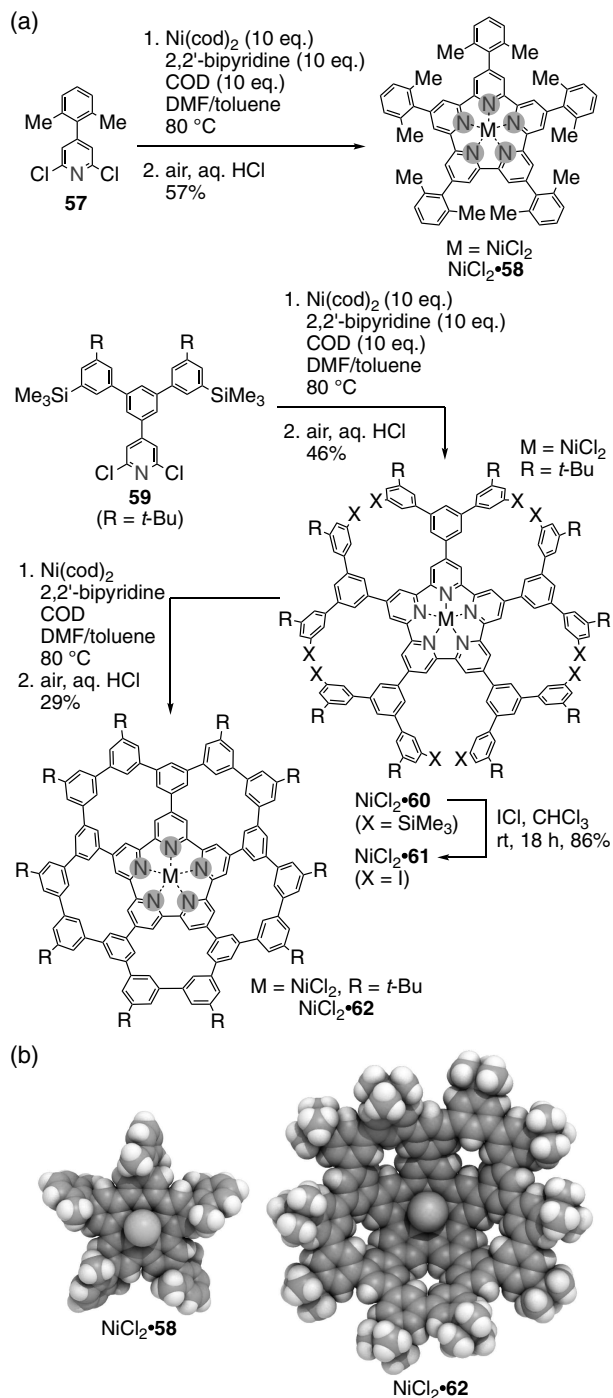


Fig. 11. (Color online) Heteroatom doping of nanocarbon molecules by metal-templated oligomeric macrocyclization via coupling (MOMC). (a) Synthesis. (b) Space-filling models show crystal structures of NiCl<sub>2</sub>•**58** and NiCl<sub>2</sub>•**62**. Chlorine atoms are shown as green balls.

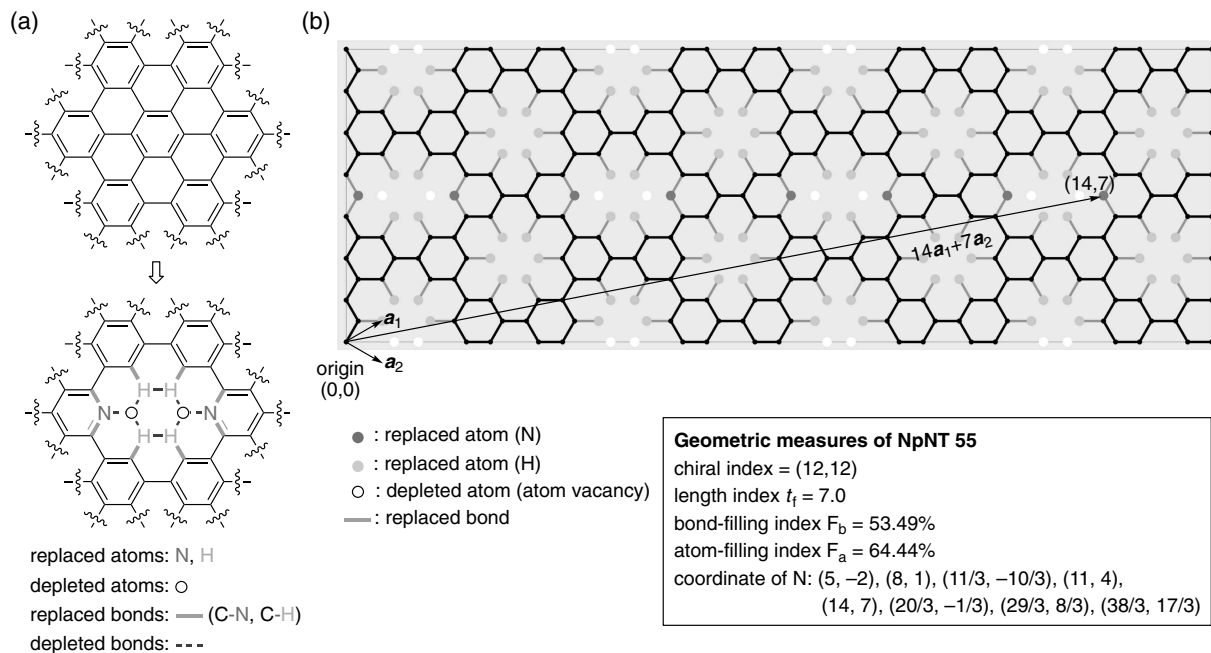


Fig. 12. (Color online) Systematic descriptors of doped finite nanotube molecules. (a) Four types of defects. (b) Representative geometric features of NpNT **55**.

indispensable. We thus decided to develop descriptors that can specify the locations of heteroatoms. Periodic honeycomb networks of CNTs are suitable for vector descriptors, and nomenclatures with unit vectors ( $\mathbf{a}_1$  and  $\mathbf{a}_2$ ) on the oblique coordinate system (OCS) have been established by physicists.<sup>70</sup> For instance, the chiral index,  $(n,m)$  from  $\mathbf{C}_h = n\mathbf{a}_1 + m\mathbf{a}_2$ , is widely accepted as a vector nomenclature to specify CNTs. We have also adopted this vector nomenclature to define the lengths of finite-length CNT molecules.<sup>49,71</sup> In the cylindrical structure of pNTs, dopants and defects were located at specific positions of parent CNTs, and systematic descriptors have been developed for their specifications/designations. When we viewed pNT/NpNT as defective, porous CNTs, four types of structural defects were observed: replaced atoms, depleted atoms, replaced bonds and depleted bonds (Fig. 12a). We noticed that the location of the defect atoms (replaced or depleted) could be specified as a unique coordinate on the OCS if the point of origin of the OCS was set. We thus set the origin at an  $sp^2$ -type atom in the edge hexagon of CNT molecules. When there are multiple candidates for the origin, the International Union of Pure and Applied Chemistry (IUPAC) priority rule can be applied to select an atom with the highest priority as the point of origin. We take NpNT **55**

as an example. As shown in Fig. 12b, 16  $sp^2$ -carbon atoms are present in the edge hexagons of **55**, and, as they are symmetrically equivalent, we can select any of them as the origin. From the selected origin, one of the nitrogen atoms is separated, for example, at  $14\mathbf{a}_1 + 7\mathbf{a}_2$ , and the coordinate, (14,7), can designate its position. Together with previous structural indices, we can specify and designate the structural features of NpNT **55** as follows: the porous CNT molecule **55** possesses a chiral index of (12,12), length index ( $t_l$ ) of 7.0, bond-filling index ( $F_b$ ) of 53.49% and atom-filling index ( $F_a$ ) of 64.44%, and the nitrogen dopants are located at (5, -2), (8,1), (11/3, -10/3), (11,4), (14,7), (20/3, -1/3), (29/3, 8/3) and (38/3, 17/3).<sup>60</sup> For convenience, we also developed and provided a web-based applet for the nomenclature of doped and porous CNT molecules.<sup>72</sup> The chemistry of doped finite nanotube molecules is still in its infancy, and we hope that this nomenclature can facilitate its development.

**5.2. Curved phenine normal vector: Pyramidalization.** Two geometric measures were introduced to quantify and describe the structural deformations of phenine networks. The first measure was the “curved phenine normal vector” (CPNV), which defines the direction of pyramidalization of the trigonal phenine panel.<sup>73</sup> This vector can be used to

quantify the degree of pyramidalization of the phenine panels and to define dihedral angles between two phenine panels. Previously, for  $sp^2$ -carbon atoms, the “ $\pi$ -orbital axis vector” (POAV) was developed to quantify the pyramidalization and dihedral angles of small curved  $\pi$ -systems,<sup>74–76</sup> but this structural measure turned out to be too fine to cover and quantify larger, nanometer-sized networks of phenines. Mimicking the definitions of POAV in a larger phenine, three  $\sigma$ -bond vectors of 1,3,5-linkages were adopted to define the CPNV ( $\mathbf{v}_p$ ) (Fig. 13). Pyramidalization angles ( $\theta$ ) and dihedral angles ( $\phi$ ) can then be derived for phenine networks. Representative

examples from crystal structures are shown in Fig. 13. Thus, the CPNV analyses can reveal locations and degrees of pyramidalized phenine panels, which can indicate the presence of local strains. The dihedral angles can also quantify the planarity of phenine networks over single-bond bridges. For instance, red-colored phenine panels of **1** and  $NiCl_2 \cdot \mathbf{62}$  with high  $\theta$  values show that strained panels of bowl-shaped phenine nanocarbons are localized at the pentagon center,<sup>34,65</sup> revealing the role of the pentagon in contorting the nanometer-sized molecular structure. The phenine panels at the center of the bowls tend to be coplanar, with small dihedral angles at the green biaryl bonds. When the phenine network is expanded with additional pentagons in the form of **4**,<sup>40</sup> the contorting effect of the central pentagon spreads over the periphery, as shown with red panels of the molecule. The  $\phi$ -value analyses of **4** also show that the structure was deformed to an oval shape, mainly due to nonplanar dihedral angles. The CPNV analyses also revealed important roles of dihedral angles in dictating the dynamic, fluctuating nanometer-scale shapes of molecules with **2** and **4**.<sup>40,42</sup> With the cylindrical phenine networks, the CPNV analyses show that N-dopants are inert to the structural distortions, showing essentially identical  $\theta$ - and  $\phi$ -distributions of pNT molecules (**5** and **55**). Although the CPNV analyses were useful for revealing local structural distortions of phenine panels, we found that they could not reveal the large-scale curvatures of molecules, which prompted us to develop the second geometric measure (see below).

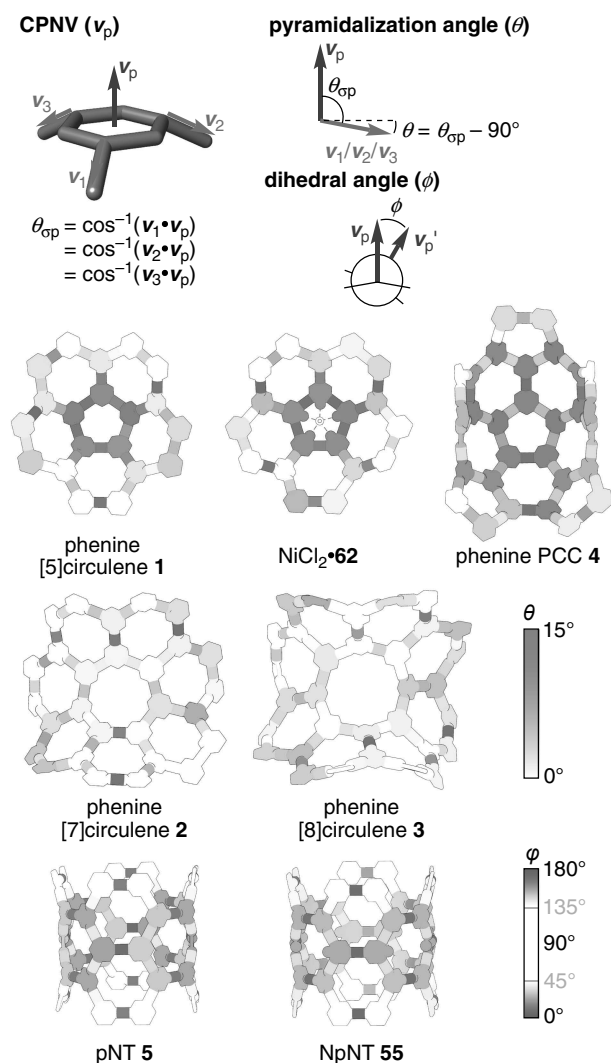


Fig. 13. (Color online) CPNV analyses of phenine nanocarbons. Representative structures of phenine nanocarbon molecules from crystal structures are shown. For  $NiCl_2 \cdot \mathbf{62}$  and NpNT **55**, nitrogen atoms are shown as ball models. See Fig. 14 for comparisons of geometry measures.

**5.3. Molecular Gauss curvature: Discrete surface theory.** “Curvature” is becoming an important notion in the study of nanocarbons,<sup>77–80</sup> and discussion and investigations of curvature in nanocarbon molecules are increasingly attracting attention. However, discussion and judgment of the curvature of molecules are often subjective, and qualitative discussion based on an “impression” of molecular shapes prevails, particularly, in the field of synthetic chemistry. On the other hand, several attempts have been made to quantitatively define the curvature of molecules by using mathematics/geometry. Among the various methods developed to date, we decided to use the discrete surface theory of Kotani, Naito and Omori, which adopted atoms and their chemical graphs as the basis for defining the molecular Gauss curvature ( $K$ ).<sup>81</sup>

As with POAV/CPNV developments, the discrete surface theory of atomic precision was found to

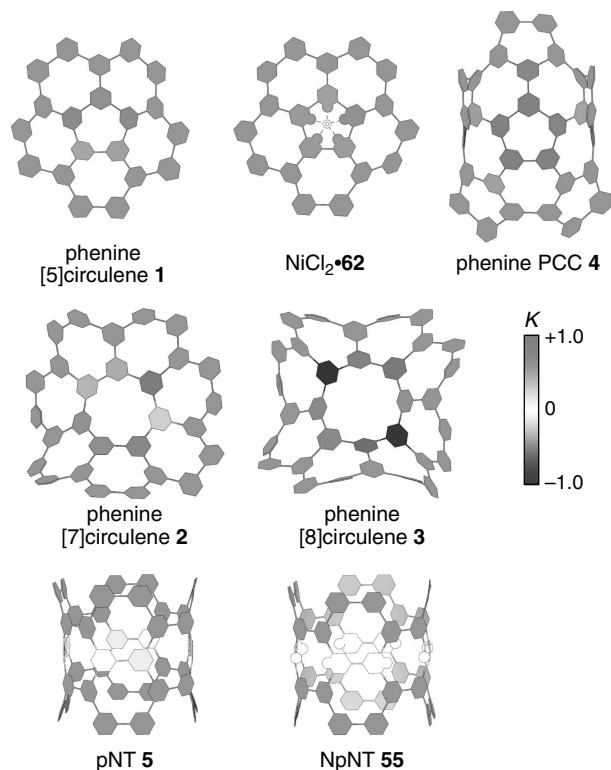


Fig. 14. (Color online) Molecular Gauss curvatures of phenine networks. For  $\text{NiCl}_2 \cdot 62$  and  $\text{NpNT } 55$ , nitrogen atoms are shown as ball models. See Fig. 13 for comparisons of geometry measures.

be too fine to reveal the curvature of a larger nanometer-sized phenine network. The theory hence was enlarged by adopting phenine as trivalent vertices,<sup>44)</sup> whereas  $\text{sp}^2$ -carbon atoms were used as the trivalent vertices in the original theory. Our method was originally developed to define and visualize the molecular Gauss curvature of phenine [8]circulene **3** and, in this paper, was applied to other representative phenine nanocarbon molecules. As shown in Fig. 14, the molecular Gauss curvature nicely depicts the curvature quantitatively, with color mapping laid over the structure. The positive Gauss curvature in the bowl-shaped nanocarbons was found at the central pentagon ( $K > 0$ ; red in Fig. 14), and by comparing with the CPNV mappings of Fig. 13, we found that pyramidalized phenine panels shaped the positive curvature of the molecules. Although CPNV analyses of [7]- and [8]circulenes of phenine (**2** and **3**) failed to allocate the characteristic of negative curvature, the molecular Gauss curvature unequivocally revealed the presence of negative curvature at the central

heptagon and octagon ( $K < 0$ ; blue in Fig. 14). The color mappings also showed that the degree of negative curvature was higher in phenine [8]circulene.

The molecular Gauss curvature nicely matches notions in mathematics/geometry, which is typically demonstrated with cylindrical molecules. Thus, as shown in the molecular Gauss curvatures of pNT (**5**) and NpNT (**55**), the molecular Gauss curvature on the cylinder was negligible ( $K \sim 0$ ; white in Fig. 14). This value,  $K = 0$ , was indeed an ideal value expected for cylinders where one of the two principal curvatures is zero. The same expectation holds for other molecules with bowl shapes and saddle shapes. Therefore, the obtained values of  $K > 0$ ,  $K < 0$  and  $K \sim 0$  for the molecular Gauss curvature quantitatively evaluate the curvature of phenine nanocarbon molecules, which matches well with our “impressions” of molecular shapes. We hope that such quantitative evaluations of the curvature can repel subjective discussion based on impressions and will deepen and accelerate the development of nanocarbon molecules.

**5.4. Structural mathematics: Stereoisomerism of phenine polluxene.** From the very beginning of the study of molecular chirality,<sup>82)–86)</sup> knowing the number of stereoisomers has been the first indispensable step for perceiving the stereoisomerism of a chiral molecule. Enumeration of stereoisomers becomes difficult when multiple chirality origins are embedded in cyclic structures, which gives rise to unique stereoisomerism known as cyclostereoisomerism.<sup>87)</sup> Although a series of anomalous cyclostereoisomerism of cycloarylenes has recently been revealed through studies of nanocarbon molecules,<sup>19),88)–90)</sup> the stereoisomerism of cyclic phenine networks is more complicated. Complicated stereoisomerism was found when the phenine networks were woven in a cage structure of phenine polluxene (**6**).<sup>52)</sup> When we found two enantiomers of **6** in a single crystal via crystallographic analyses (see above), important questions about its stereoisomerism emerged: “Are there only two enantiomeric structures available for **6** (Fig. 15)? If no, how many isomeric structures are possible with this uniquely fused cage?” Although these simple questions turned out to be difficult, particularly for organic chemists, an answer was obtained with the aid of structural mathematics. The cage structure of **6** possesses 15 biaryl bonds, and by considering the (*R*)/(*S*)-configurations available for each bond, we could count  $2^{15} = 32768$  isomers from redundant combinations. Cyclostereoisomerism requires careful consideration

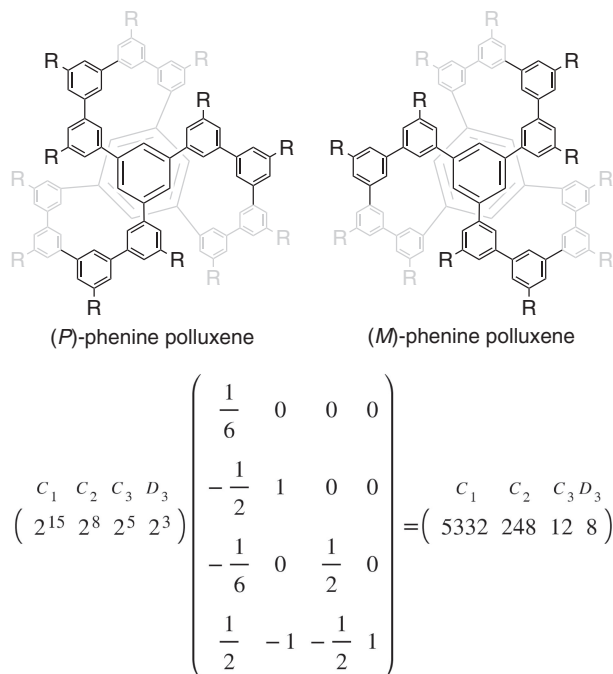


Fig. 15. Stereoisomerism and structural mathematics of phenine polluxene.

of the degeneracies of isomeric structures, but manual examinations of these 32768 combinations were naturally impossible. Eventually, we found that a method developed from Pólya's theorem could give answers.<sup>91,92)</sup> The fused cage structure of **6** had  $D_3$  point symmetry, which should have a nonredundant set of subgroups of ( $C_1$ ,  $C_2$ ,  $C_3$ ,  $D_3$ ). By counting possible isomers for each symmetry subgroup, the actual figures for the subgroups were ( $2^{15}$ ,  $2^8$ ,  $2^5$ ,  $2^3$ ). The number of isomers for each subgroup could be derived by applying the inverse of the table of marks for  $D_3$  point symmetry (Fig. 15), which results in the total number of isomers being  $5332 + 248 + 12 + 8 = 5600$ . This symmetry-based enumeration method seems to be versatile, which may help chemists resolve and explore novel stereoisomerism.

## 6. Molecular assembly

Studies on the molecular assembly of phenine [ $n$ ]circulenes deepened our understanding of the characteristics of large, nanometer-sized  $\pi$ -surfaces. Upon crystallization, phenine [ $n$ ]circulene molecules commonly formed stacked dimers by matching curved surfaces as shown in Fig. 16. Solution-phase analyses by  $^1\text{H}$  NMR spectroscopy also revealed the presence of dimers. For instance, phenine [5]circulene **1** showed two sets of resonances originating from

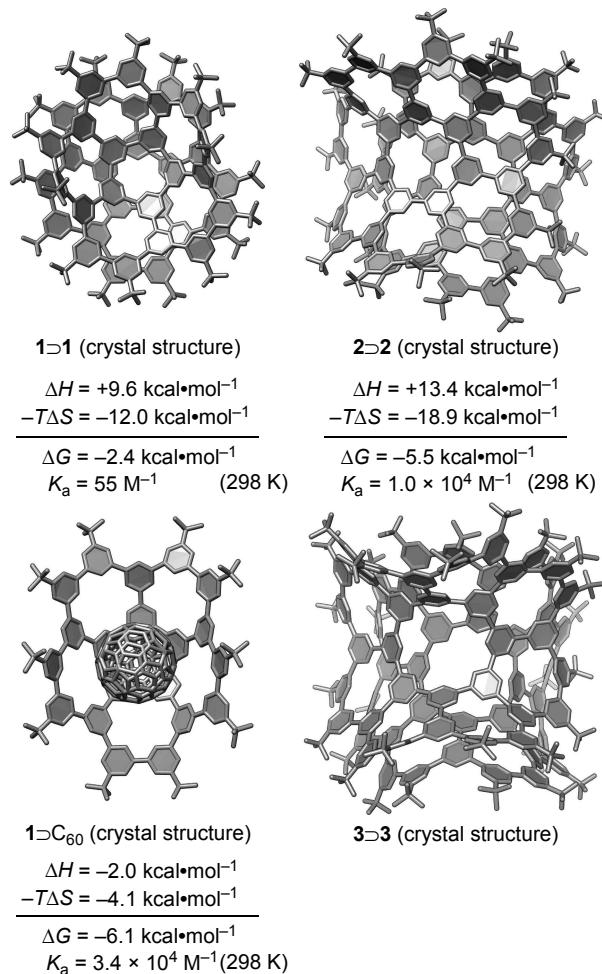


Fig. 16. (Color online) Molecular assembly of phenine nanocarbons. Representative crystal structures and thermodynamic parameters are shown.

monomeric and dimeric species, which were fully characterized by diffusion-ordered spectroscopy (DOSY).<sup>34)</sup> Unexpectedly, upon elevating the analysis temperature, the population of dimers increased. Detailed van't Hoff analysis of the VT NMR spectra revealed that the dimeric assembly was purely driven by entropy. The association constant of  $55 \text{ M}^{-1}$  was recorded in  $\text{CDCl}_3$  at 298 K, but the association was enthalpically disfavored by  $\Delta H = +9.6 \text{ kcal}\cdot\text{mol}^{-1}$ . The assembly was made possible by favorable entropy contributions of  $-T\Delta S = -12.0 \text{ kcal}\cdot\text{mol}^{-1}$  (298 K). The entropy-driven assembly was likewise observed with phenine [7]circulene **2** with  $\Delta H = +13.4 \text{ kcal}\cdot\text{mol}^{-1}$  and  $-T\Delta S = -18.9 \text{ kcal}\cdot\text{mol}^{-1}$  (298 K) for a  $K_a$  value of  $1.0 \times 10^4 \text{ M}^{-1}$  in  $\text{CDCl}_3$ .<sup>42)</sup> Although a single species was observed with phenine

[8]circulene **3**, the DOSY analyses confirmed it to be dimeric assembly. The monomeric species was not observed even at 0.003 mM,<sup>44)</sup> which indicated a large association constant of  $K_a > 10^8 \text{ M}^{-1}$ .<sup>§§</sup> Although the enthalpy contribution was favorably altered, host-guest assembly of phenine [5]circulene with  $\text{C}_{60}$  was largely driven by entropy.<sup>93)</sup> We believe that “entropy-driven assembly” should be characteristics of large nanocarbons, which could be ascribed to unique desolvation dynamics at the contorted  $\pi$ -surfaces.<sup>94)</sup>

## 7. Defects and dopants

### 7.1. Defects and dopants in cylinders.

Atomic-level controls of the electronic characteristics of nanocarbons attract much attention and are often taken up as subjects of theoretical studies. However, defects/dopants cannot be possibly located at specific positions with atomic precision for the nanocarbons produced by physical methods, which hampers in-depth understanding of the effects of these structural anomalies. We realized that the effects of structural anomalies could be examined with cylindrical congeners of phenine nanocarbons, *i.e.*, pNTs, which were ideal for the first structure-property relationship studies. The pNT molecules investigated were **5**, **55** and **56** (see Figs. 2, 7 and 10 for the molecular structures).

Our pNT molecule (**5**) is a segment of (12,12)-CNT having a length index ( $t_f$ ) of 7.0 with bond- and atom-filling indices of 56.59% and 66.67%, respectively.<sup>51)</sup> The defects of **5** are composed of deletions and replacements of carbon atoms, which are periodically distributed over the cylinder.<sup>\*\*\*</sup> The bandgap was theoretically calculated as 3.73 eV, which only differed by 1.05 eV from its infinite congener (Fig. 17). These bandgaps can be typical features of defective CNTs, as parent, nondefective armchair CNTs with a chiral index of ( $n,n$ ) are considered metallic with no bandgap between the valence and conduction bands.<sup>70)</sup>

Heteroatom dopants allowed for further band-gap manipulations, which was demonstrated with nitrogen-doped pNTs (**55**, **56**).<sup>60,64)</sup> As seen from the theoretical analyses of electronic structures of **55**

(Fig. 17), pyridinic nitrogen dopants inserted low-lying vacant orbitals on the conduction band side of pNT and narrowed the gap to 3.07 eV. When pyrrolic nitrogen atoms were further doped at the edge of the cylinder in the form of **56**, high-energy filled orbitals were inserted, which resulted in further narrowing of the gap to 2.00 eV. Previously, with infinite N-doped CNTs, the roles of nitrogen dopants were extensively studied and discussed.<sup>61)–63)</sup> However, because of the lack of atomically defined congeners, correlating the properties of CNTs with atomic-level structures has been difficult, and discussion of the dopant effect has long been controversial. The present studies revealed the roles of pyridinic and pyrrolic nitrogen atoms as acceptors and donors, respectively, which was also confirmed by experimental observation. When the luminescence of NpNT **56** was investigated (Fig. 17b), a substantial bathochromic shift was observed, in accordance with the increasing polarity of the solvents (Fig. 17b). The solvent-dependent bathochromic shift was absent for NpNT **55**, which led us to conclude that the solvatochromism was due to intramolecular charge transfer from pyrrole to pyridine. The preceding observations of twisted intramolecular charge transfer (TICT) with simpler compounds confirmed this conclusion.<sup>95)</sup>

**7.2. Transition-metal dopants.** The phenine design allowed us to introduce unpaired electrons into nanocarbon molecules, as demonstrated by COPy-5 complexes with paramagnetic Ni(II) (see also Section 4.2).<sup>65)</sup> The macrocyclic systems endowed the Ni(II) center with a unique pentagonal bipyramidal coordination, which was attributed to the high-spin state of the metal. Paramagnetic NMR spectra of Ni(II)-COPy-5 complexes ( $\text{NiCl}_2 \cdot \mathbf{58}$  and

§§ Considering that the monomer abundance was less than 5% at 0.003 mM, we may roughly estimate the association constant for the dimer of **3** as  $>2 \times 10^8 \text{ M}^{-1}$ . In previous study (Ref. 42), we estimated  $\Delta H/\Delta S$  values per phenine unit from thermodynamic parameters of phenine [5]- and [7]circulenes. However, the data of phenine [8]circulene suggested that the values could deviate with the larger congener, requiring further detailed investigations.

\*\*\* Coordinates of replaced atoms (H): (2,0), (2,1), (2,-2), (4/3,1/3), (4,1), (4,-2), (5,0), (5,1), (5,3), (5,4), (5,-2), (5,-3), (5,-5), (7/3,1/3), (7,1), (7,4), (7,-2), (7,-5), (8,0), (8,1), (8,3), (8,4), (8,6), (8,7), (8,-2), (8,-3), (8,-5), (10,1), (10,4), (10,7), (10,-2), (11,0), (11,1), (11,3), (11,4), (11,6), (11,7), (11,9), (11,10), (11,-2), (13/3,1/3), (13/3,4/3), (13/3,10/3), (13/3,-5/3), (13/3,-8/3), (13,1), (13,4), (13,7), (13,10), (14,1), (14,3), (14,4), (14,6), (14,7), (14,9), (14,10), (16/3,1/3), (16/3,10/3), (16/3,-8/3), (16,4), (16,7), (17,4), (17,6), (17,7), (22/3,1/3), (22/3,4/3), (22/3,10/3), (22/3,13/3), (22/3,19/3), (22/3,-5/3), (22/3,-8/3), (22/3,-14/3), (22/3,-17/3), (25/3,1/3), (25/3,10/3), (25/3,19/3), (25/3,-8/3), (31/3,1/3), (31/3,4/3), (31/3,10/3), (31/3,13/3), (31/3,19/3), (31/3,22/3), (31/3,28/3), (31/3,-5/3), (31/3,-8/3), (34/3,1/3), (34/3,10/3), (34/3,19/3), (34/3,28/3), (40/3,1/3), (40/3,4/3), (40/3,10/3), (40/3,13/3), (40/3,19/3), (40/3,22/3), (40/3,28/3), (40/3,31/3), (43/3,10/3), (43/3,19/3), (43/3,28/3), (49/3,10/3), (49/3,13/3), (49/3,19/3), (49/3,22/3), (52/3,19/3); coordinates of depleted atoms: (1,1), (4/3,4/3), (4,4), (7,7), (8,-6), (10,10), (11,-3), (13/3,13/3), (14,0), (17,3), (22/3,22/3), (25/3,-17/3), (31/3,31/3), (34/3,-8/3), (43/3,1/3), (52/3,10/3).

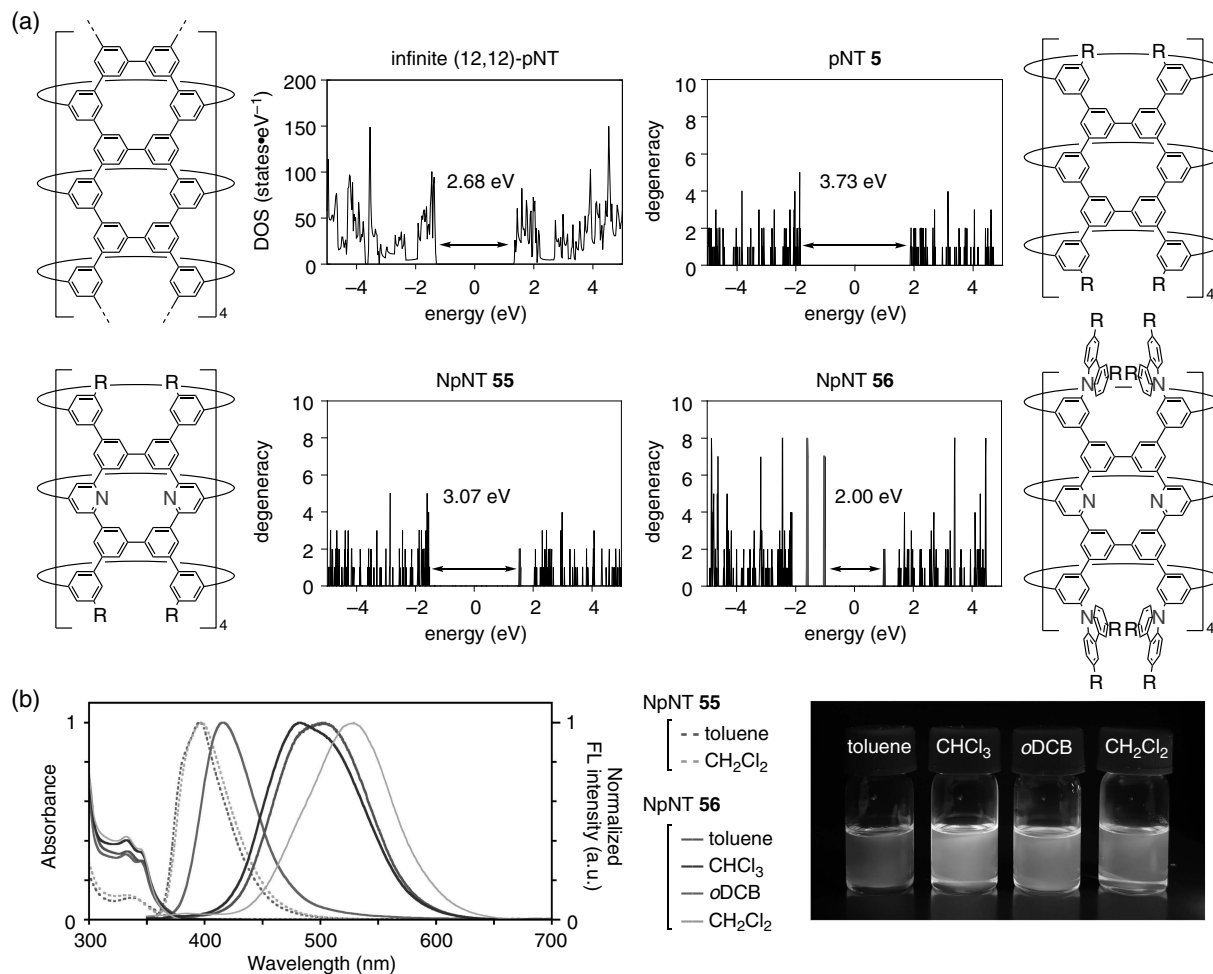


Fig. 17. (Color online) Manipulations of electronic structures of nanotubes with defects and dopants. (a) Density of states of infinite (12,12)-pNT and histograms sorting molecular orbitals of pNT **5** and NpNTs **55** and **56** (PBEPBE/STO-3G).<sup>51),60),64)</sup> For comparison, the midgap energies are set to zero. For NpNTs **55** and **56**, pyridinic  $\pi^*$ -orbitals and carbazolyl  $\pi$ -orbitals are colored blue and red, respectively. (b) Absorption and photoluminescence spectra of NpNTs **55** and **56**.<sup>64)</sup> A photograph of the photoluminescence of **56** in various solvents under irradiation at 365 nm is also shown.

NiCl<sub>2</sub>•**62**) showed the effect of interactions of the unpaired electrons with nanocarbon systems. The most notable feature was the large paramagnetic shifts observed with <sup>1</sup>H and <sup>13</sup>C resonances. For example, two <sup>13</sup>C resonances of **62** appeared at anomalous positions of 352 ppm and 22 ppm (Fig. 18), confirming the occurrence of hyperfine interactions between the carbon nuclei and unpaired electrons.<sup>96)</sup> The unpaired electrons also provided efficient relaxation pathways for <sup>13</sup>C nuclear spins, which dramatically shortened the spin-lattice relaxation time ( $T_1$ ). Distributions of the spin density over nanocarbon molecules, as well as their applications, are of interest for further in-depth studies.

## 8. Conclusion

Facing ever-increasing numbers of novel organic molecules, we may find truth in the remarks of Laurent<sup>5)</sup>: “the chemistry of carbon differs from mineral chemistry by the unlimited number of combinations which may be produced... organic chemistry will appear to us inaccessible, from the infinite number of substances which it embraces, the catalogue of which will shortly exceed that elaborated by astronomers for the stars themselves”. Fueled by the discoveries of nanocarbons, organic chemists today have started to design novel nanocarbon “molecules”, and the structural library of nanocarbon molecules is now rapidly growing. Consequently,

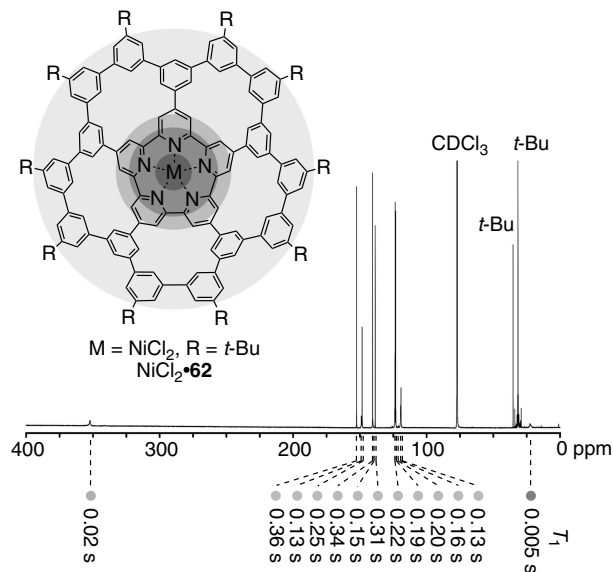


Fig. 18. (Color online) High-spin transition-metal dopant at the center of the N-doped phenine nanocarbon. The  $^{13}\text{C}$  NMR spectrum of  $\text{NiCl}_2\cdot\mathbf{62}$  is shown with  $T_1$  values.

another labyrinth may seem to emerge, particularly, in “the absence of all system, all nomenclature, for the classification and denomination of this multitude of bodies”.<sup>5)</sup> Hoping to deepen our understanding of nanocarbons with a simple language of molecular science, *i.e.*, chemistry, we launched our explorations of phenine nanocarbon molecules. Laurent found that “organic chemistry becomes at once remarkably simplified”, once systems for the classification and denomination were created and developed. We believe that systematic syntheses as well as classification and denomination of thus created simple yet large nanocarbon molecules can cast light to direct us in the nanocarbon labyrinth. We hope to contribute to its developments by our explorations of phenine nanocarbons. As summarized in this account, the developments during the first half a decade were mostly synthetic, which allowed for systematic, rapid explorations of novel nanometer-sized structures. Assembling  $6\pi$  phenine units, we can readily access unique nanocarbon molecules with contorted,  $\pi$ -rich structures that are also decorated by structural defects, lone-pair n-electrons and/or transition-metal d-electrons located at specific positions. Tools were also provided to define and describe the structural features of nanocarbon molecules, which, we hope, can simplify the chemistry discussion of nanocarbon molecules. We wish to continue our endeavor in expanding the scope of phenine nano-

carbons and hope that studies on their properties and applications will help us to deepen our understanding of nanocarbons.

### Acknowledgments

The authors wish to express their appreciation for all the coauthors and supporters whose names appear in the original papers. This work is partly supported by KAKENHI (20H05672 and 22H02059).

### References

- 1) Laurent, A. (1836) Sur la chlorophénise et les acides chlorophénisique et chlorophénèsique. *Ann. Chim. Phys.* **63**, 27–45.
- 2) Kapoor, S.C. (1969) The origins of Laurent’s organic classification. *Isis* **60**, 477–527.
- 3) Faraday, M. (1825) XX. On new compounds of carbon and hydrogen, and on certain other products obtained during the decomposition of oil by heat. *Philos. Trans. R. Soc.* **115**, 440–466.
- 4) Kaiser, R. (1968) “Bicarburet of hydrogen”. Reappraisal of the discovery of benzene in 1825 with the analytical methods of 1968. *Angew. Chem. Int. Ed. Engl.* **7**, 345–350.
- 5) Laurent, A. (1855) *Chemical Method, Notation, Classification, & Nomenclature*. Cavendish Society, London.
- 6) Fabre, H.A. and Powell, W.H. (2013) *Nomenclature of Organic Chemistry: IUPAC Recommendations and Preferred Names 2013*. The Royal Chemical Society, Cambridge.
- 7) Nickon, A. and Silversmith, E.F. (1987) *Organic Chemistry, the Name Game: Modern Coined Terms and their Origins*. Pergamon Press, New York.
- 8) Barth, W.E. and Lawton, R.G. (1966) Dibenzo[*ghi,mno*]fluoranthene. *J. Am. Chem. Soc.* **88**, 380–381.
- 9) Scott, L.T., Hashemi, M.M., Meyer, D.T. and Warren, H.B. (1991) Corannulene. A convenient new synthesis. *J. Am. Chem. Soc.* **113**, 7082–7084.
- 10) Butterfield, A.M., Gilomen, B. and Siegel, J.S. (2012) Kilogram-scale production of corannulene. *Org. Process Res. Dev.* **16**, 664–676.
- 11) Osawa, E. (1970) Superaromaticity. *Kagaku* **25**, 854–863.
- 12) Curl, R.F., Smalley, R.E., Kroto, H.W., O’Brien, S. and Heath, J.R. (2001) How the news that we were not the first to conceive of soccer ball  $\text{C}_{60}$  got to us. *J. Mol. Graph. Model.* **19**, 185–186.
- 13) Kroto, H.W., Heath, J.R., O’Brien, S.C., Curl, R.F. and Smalley, R.E. (1985)  $\text{C}_{60}$ : Buckminsterfullerene. *Nature* **318**, 162–163.
- 14) Iijima, S. (1991) Helical microtubules of graphitic carbon. *Nature* **354**, 56–58.
- 15) IUPAC. (1997) Molecular entity. *In Compendium of Chemical Terminology*, 2nd ed. (the “Gold Book”). Compiled by McNaught, A.D. and Wilkinson, A. Blackwell Scientific Publications, Oxford (1997).

- Online version (2019–) created by Chalk, S.J. <https://doi.org/10.1351/goldbook>.
- 16) Yamamoto, K., Harada, T., Nakazaki, M., Naka, T., Kai, Y., Harada, S. *et al.* (1983) Synthesis and characterization of [7]circulene. *J. Am. Chem. Soc.* **105**, 7171–7172.
  - 17) Feng, C.-N., Kuo, M.-Y. and Wu, Y.-T. (2013) Synthesis, structural analysis, and properties of [8]circulenes. *Angew. Chem. Int. Ed.* **52**, 7791–7794.
  - 18) Sakamoto, Y. and Suzuki, T. (2013) Tetrabenzo[8]-circulene: Aromatic saddles from negatively curved graphene. *J. Am. Chem. Soc.* **135**, 14074–14077.
  - 19) Sun, Z., Matsuno, T. and Isobe, H. (2018) Stereoisomerism and structures of rigid cylindrical cycloarylenes. *Bull. Chem. Soc. Jpn.* **91**, 907–921.
  - 20) Ikemoto, K. and Isobe, H. (2021) Geodesic phenine frameworks. *Bull. Chem. Soc. Jpn.* **94**, 281–294.
  - 21) Miyaura, N. (2002) Cross-Coupling Reactions: A Practical Guide; Topics in Current Chemistry (Topics in Current Chemistry, Vol. 219). Springer-Verlag, Heidelberg.
  - 22) Miyaura, N., Yamada, K. and Suzuki, A. (1979) A new stereospecific cross-coupling by the palladium-catalyzed reaction of 1-alkenylboranes with 1-alkenyl or 1-alkynyl halides. *Tetrahedron Lett.* **20**, 3437–3440.
  - 23) Yamamoto, T., Hayashi, Y. and Yamamoto, A. (1978) A novel type of polycondensation utilizing transition metal-catalyzed C–C coupling. I. Preparation of thermostable polyphenylene type polymers. *Bull. Chem. Soc. Jpn.* **51**, 2091–2097.
  - 24) Fuhrmann, G., Debaerdemaeker, T. and Bäuerle, P. (2003) C–C bond formation through oxidatively induced elimination of platinum complexes—A novel approach towards conjugated macrocycles. *Chem. Commun.* 948–949.
  - 25) Yamago, S., Watanabe, Y. and Iwamoto, T. (2010) Synthesis of [8]cycloparaphenylene from a square-shaped tetranuclear platinum complex. *Angew. Chem. Int. Ed.* **49**, 757–759.
  - 26) Hitosugi, S., Nakanishi, W., Yamasaki, T. and Isobe, H. (2011) Bottom-up synthesis of finite models of helical (*n,m*)-single-wall carbon nanotubes. *Nat. Commun.* **2**, 492.
  - 27) Miyake, Y., Wu, M., Rahman, M.J., Kuwatani, Y. and Iyoda, M. (2006) Efficient construction of biaryls and macrocyclic cyclophanes via electron-transfer oxidation of Lipshutz cuprates. *J. Org. Chem.* **71**, 6110–6117.
  - 28) Nakanishi, W., Yoshioka, T., Taka, H., Xue, J.Y., Kita, H. and Isobe, H. (2011) [*n*]Cyclo-2,7-naphthylenes: Synthesis and isolation of macrocyclic aromatic hydrocarbons having bipolar carrier transport ability. *Angew. Chem. Int. Ed.* **50**, 5323–5326.
  - 29) Xue, J.Y., Ikemoto, K., Takahashi, N., Izumi, T., Taka, H., Kita, H. *et al.* (2014) Cyclo-*meta*-phenylene revisited: Nickel-mediated synthesis, molecular structures, and device applications. *J. Org. Chem.* **79**, 9735–9739.
  - 30) Ikemoto, K., Yoshii, A., Izumi, T., Taka, H., Kita, H., Xue, J.Y. *et al.* (2016) Modular synthesis of aromatic hydrocarbon macrocycles for simplified, single-layer organic light-emitting devices. *J. Org. Chem.* **81**, 662–666.
  - 31) Ishiyama, T., Takagi, J., Ishida, K., Miyaura, N., Anastasi, N.R. and Hartwig, J.F. (2002) Mild iridium-catalyzed borylation of arenes. High turnover numbers, room temperature reactions, and isolation of a potential intermediate. *J. Am. Chem. Soc.* **124**, 390–391.
  - 32) Mkhaliid, I.A.I., Barnard, J.H., Marder, T.B., Murphy, J.M. and Hartwig, J.F. (2010) C-H activation for the construction of C-B bonds. *Chem. Rev.* **110**, 890–931.
  - 33) Hitosugi, S., Nakamura, Y., Matsuno, T., Nakanishi, W. and Isobe, H. (2012) Iridium-catalyzed direct borylation of phenacenes. *Tetrahedron Lett.* **53**, 1180–1182.
  - 34) Ikemoto, K., Kobayashi, R., Sato, S. and Isobe, H. (2017) Synthesis and bowl-in-bowl assembly of a geodesic phenylene bowl. *Angew. Chem. Int. Ed.* **56**, 6511–6514.
  - 35) Boorum, M.M., Vasil'ev, Y.V., Drewello, T. and Scott, L.T. (2001) Groundwork for a rational synthesis of C<sub>60</sub>: Cyclodehydrogenation of a C<sub>60</sub>H<sub>30</sub> polyarene. *Science* **294**, 828–831.
  - 36) Scott, L.T., Boorum, M.M., McMahan, B.J., Hagen, S., Mack, J., Blank, J. *et al.* (2002) A rational chemical synthesis of C<sub>60</sub>. *Science* **295**, 1500–1503.
  - 37) Scott, L.T. (2004) Methods for the chemical synthesis of fullerenes. *Angew. Chem. Int. Ed.* **43**, 4994–5007.
  - 38) Geneste, F., Moradpour, A., Dive, G., Peeters, D., Malthête, J. and Sadoc, J.-F. (2002) Retrosynthetic analysis of fullerene C<sub>60</sub>: Structure, stereochemistry, and calculated stability of C<sub>30</sub> fragments. *J. Org. Chem.* **67**, 605–607.
  - 39) Richaud, A., López, M.J., Mojica, M., Alonso, J.A. and Méndez, F. (2020) Dimerization of pentacyclopentacorannulene C<sub>30</sub>H<sub>10</sub> as a strategy to produce C<sub>60</sub>H<sub>20</sub> as a precursor for C<sub>60</sub>. *RSC Adv.* **10**, 3689–3693.
  - 40) Mio, T., Ikemoto, K., Sato, S. and Isobe, H. (2020) Synthesis of a hemispherical geodesic phenine framework by a polygon assembling strategy. *Angew. Chem. Int. Ed.* **59**, 6567–6571.
  - 41) Smalley, R.E. (1992) Self-assembly of the fullerenes. *Acc. Chem. Res.* **25**, 98–105.
  - 42) Ikemoto, K., Lin, J., Kobayashi, R., Sato, S. and Isobe, H. (2018) Fluctuating carbonaceous networks with a persistent molecular shape: A saddle-shaped geodesic framework of 1,3,5-trisubstituted benzene (phenine). *Angew. Chem. Int. Ed.* **57**, 8555–8559.
  - 43) IUPAC. (1997) Congener. *In* Compendium of Chemical Terminology, 2nd ed. (the “Gold Book”). Compiled by McNaught, A.D. and Wilkinson, A. Blackwell Scientific Publications, Oxford (1997). Online version (2019–) created by Chalk, S.J. <https://doi.org/10.1351/goldbook>.
  - 44) Ikemoto, K., Akiyoshi, M., Mio, T., Nishioka, K., Sato, S. and Isobe, H. (2022) Synthesis of a

- negatively curved nanocarbon molecule with an octagonal omphalos via design-of-experiments optimizations supplemented by machine learning. *Angew. Chem. Int. Ed.* **61**, e202204035.
- 45) Lewis, S.E. (2015) Cycloparaphenylenes and related nanohoops. *Chem. Soc. Rev.* **44**, 2221–2304.
- 46) Darzi, E.R. and Jasti, R. (2015) The dynamic, size-dependent properties of [5]–[12]cycloparaphenylenes. *Chem. Soc. Rev.* **44**, 6401–6410.
- 47) Segawa, Y., Yagi, A., Matsui, K. and Itami, K. (2016) Design and synthesis of carbon nanotube segments. *Angew. Chem. Int. Ed.* **55**, 5136–5158.
- 48) Yamago, S., Kayahara, E. and Iwamoto, T. (2014) Organoplatinum-mediated synthesis of cyclic  $\pi$ -conjugated molecules: Towards a new era of three-dimensional aromatic compounds. *Chem. Rec.* **14**, 84–100.
- 49) Matsuno, T., Naito, H., Hitosugi, S., Sato, S., Kotani, M. and Isobe, H. (2014) Geometric measures of finite carbon nanotube molecules: A proposal for length index and filling indexes. *Pure Appl. Chem.* **86**, 489–495.
- 50) Sun, Z., Mio, T., Ikemoto, K., Sato, S. and Isobe, H. (2019) Synthesis, structures, and assembly of geodesic phenine frameworks with isorecticular networks of [n]cyclo-*para*-phenylenes. *J. Org. Chem.* **84**, 3500–3507.
- 51) Sun, Z., Ikemoto, K., Fukunaga, T.M., Koretsune, T., Arita, R., Sato, S. *et al.* (2019) Finite phenine nanotubes with periodic vacancy defects. *Science* **363**, 151–155.
- 52) Fukunaga, T.M., Kato, T., Ikemoto, K. and Isobe, H. (2022) A minimal cage of a diamond twin with chirality. *Proc. Natl. Acad. Sci. U.S.A.* **119**, e2120160119.
- 53) Sunada, T. (2008) Crystals that nature might miss creating. *Not. Am. Math. Soc.* **55**, 208–215.
- 54) Nikerov, M.V., Bochvar, D.A. and Stankevich, I.V. (1982) Allotropic modifications of carbon. *J. Struct. Chem.* **23**, 150–152.
- 55) Itoh, M., Kotani, M., Naito, H., Sunada, T., Kawazoe, Y. and Adschiri, T. (2009) New metallic carbon crystal. *Phys. Rev. Lett.* **102**, 055703.
- 56) Yao, Y., Tse, J.S., Sun, J., Klug, D.D., Martoňák, R. and Itaka, T. (2009) Comment on “new metallic carbon crystal”. *Phys. Rev. Lett.* **102**, 229601.
- 57) Yi, J.-Y. and Bernholc, J. (1993) Atomic structure and doping of microtubules. *Phys. Rev. B* **47**, 1708–1711.
- 58) Stephan, O., Ajayan, P.M., Colliex, C., Redlich, P., Lambert, J.M., Bernier, P. *et al.* (1994) Doping graphitic and carbon nanotube structures with boron and nitrogen. *Science* **266**, 1683–1685.
- 59) Terrones, M., Grobert, N., Olivares, J., Zhang, J.P., Terrones, H., Kordatos, K. *et al.* (1997) Controlled production of aligned-nanotube bundles. *Nature* **388**, 52–55.
- 60) Ikemoto, K., Yang, S., Naito, H., Kotani, M., Sato, S. and Isobe, H. (2020) A nitrogen-doped nanotube molecule with atom vacancy defects. *Nat. Commun.* **11**, 1807.
- 61) Ayala, P., Arenal, R., Rümmeli, M., Rubio, A. and Pichler, T. (2010) The doping of carbon nanotubes with nitrogen and their potential applications. *Carbon* **48**, 575–586.
- 62) Ćirić-Marjanović, G., Pašti, I. and Mentus, S. (2015) One-dimensional nitrogen-containing carbon nanostructures. *Prog. Mater. Sci.* **69**, 61–182.
- 63) Inagaki, M., Toyoda, M., Soneda, Y. and Morishita, T. (2018) Nitrogen-doped carbon materials. *Carbon* **132**, 104–140.
- 64) Ikemoto, K., Harada, S., Yang, S., Matsuno, T. and Isobe, H. (2022) A defective nanotube molecule of C<sub>552</sub>H<sub>496</sub>N<sub>24</sub> with pyridinic and pyrrolic nitrogen atoms. *Angew. Chem. Int. Ed.* **61**, e202114305.
- 65) Yang, S., Miyachi, A., Matsuno, T., Muto, H., Sasakawa, H., Ikemoto, K. *et al.* (2021) Metal-templated oligomeric macrocyclization via coupling for metal-doped  $\pi$ -systems. *J. Am. Chem. Soc.* **143**, 15017–15021.
- 66) Xue, J.Y., Ikemoto, K., Sato, S. and Isobe, H. (2016) Introduction of nitrogen atoms in [n]cyclo-*meta*-phenylenes via cross-coupling macrocyclization. *Chem. Lett.* **45**, 676–678.
- 67) Watts, H. (1879) Appendix III. Instruction to abstractors. *J. Chem. Soc. Trans.* **35**, 276–281.
- 68) Allan, J., Oxford, A.E., Robinson, R. and Smith, J.C. (1926) LII.—The relative directive powers of groups of the forms RO and RR'N in aromatic substitution. Part IV. A discussion of the observations recorded in parts I, II, and III. *J. Chem. Soc.* **129**, 401–411.
- 69) Ingold, C.K. and Ingold, E.H. (1926) CLXIX.—The nature of the alternating effect in carbon chains. Part V. A discussion of aromatic substitution with special reference to the respective roles of polar and non-polar dissociation; and a further study of the relative directive efficiencies of oxygen and nitrogen. *J. Chem. Soc.* **129**, 1310–1328.
- 70) Saito, R., Dresselhaus, G. and Dresselhaus, M.S. (1998) *Physical Properties of Carbon Nanotubes*. Imperial College Press, London.
- 71) Geometric measurement of finite SWNT molecules (length). <http://www.chem.s.u-tokyo.ac.jp/users/physorg/finite/>.
- 72) Geometric measurement of finite SWNT molecules (defect). <https://physorg.chem.s.u-tokyo.ac.jp/applet/defect/>.
- 73) Mio, T., Ikemoto, K. and Isobe, H. (2020) Curved phenine normal vectors: Geometric measures of geodesic phenine frameworks. *Chem. Asian J.* **15**, 1355–1359.
- 74) Haddon, R.C. and Scott, L.T. (1986)  $\pi$ -Orbital conjugation and rehybridization in bridged annulenes and deformed molecules in general:  $\pi$ -Orbital axis vector analysis. *Pure Appl. Chem.* **58**, 137–142.
- 75) Haddon, R.C. (1988)  $\pi$ -Electrons in three dimensions. *Acc. Chem. Res.* **21**, 243–249.
- 76) Haddon, R.C. (1993) Chemistry of the fullerenes: The manifestation of strain in a class of continuous aromatic molecules. *Science* **261**, 1545–1550.
- 77) Cariglia, M., Giambò, R. and Perali, A. (2017) Curvature-tuned electronic properties of bilayer

- graphene in an effective four-dimensional space-time. *Phys. Rev. B* **95**, 245426.
- 78) Gao, Z., Wang, S., Berry, J., Zhang, Q., Gebhardt, J., Parkin, W.M. *et al.* (2020) Large-area epitaxial growth of curvature-stabilized ABC trilayer graphene. *Nat. Commun.* **11**, 546.
- 79) Dong, F., Wu, M., Zhang, G., Liu, X., Rawach, D., Tavares, A.C. *et al.* (2020) Defect engineering of carbon-based electrocatalysts for rechargeable zinc-air batteries. *Chem. Asian J.* **15**, 3737–3751.
- 80) Cariglia, M., Giambò, R. and Perali, A. (2018) Electronic properties of curved few-layers graphene: A geometrical approach. *Condens. Matter* **3**, 11.
- 81) Kotani, M., Naito, H. and Omori, T. (2017) A discrete surface theory. *Comput. Aided Geom. Des.* **58**, 24–54.
- 82) Gal, J. (2013) Molecular chirality in chemistry and biology: Historical milestones. *Helv. Chim. Acta* **96**, 1617–1657.
- 83) Pasteur, L. (1848) Recherches sur les relations qui peuvent exister entre la forme cristalline, la composition chimique et le sens de la polarisation rotatoire. *Ann. Chim. Phys.* **24**, 442–459.
- 84) van't Hoff, J.H. (1874) Sur les formules de structure dans l'espace. *Archives Néerlandaises des Sciences exactes et naturelles.* **9**, 445–454.
- 85) Le Bel, J.A. (1874) Sur les relations qui existent entre les formules atomiques des corps organiques et le pouvoir rotatoire de leurs dissolutions. *Bull. Soc. Chim. Fr.* **22**, 337–347.
- 86) Fischer, E. (1891) Ueber die Configuration des Traubenzuckers und seiner Isomeren. *Ber. Dtsch. Chem. Ges.* **24**, 1836–1845.
- 87) Eliel, E.L. and Wilen, S.H. (1994) Stereochemistry of organic compounds. Wiley, New York.
- 88) Sun, Z., Suenaga, T., Sarkar, P., Sato, S., Kotani, M. and Isobe, H. (2016) Stereoisomerism, crystal structures, and dynamics of belt-shaped cyclo-naphthylenes. *Proc. Natl. Acad. Sci. U.S.A.* **113**, 8109–8114.
- 89) Sarkar, P., Sun, Z., Tokuhira, T., Kotani, M., Sato, S. and Isobe, H. (2016) Stereoisomerism in nanohoops with heterogeneous biaryl linkages of *E/Z*- and *R/S*-geometries. *ACS Cent. Sci.* **2**, 740–747.
- 90) Matsuno, T., Yang, Y., Nanjo, Y., Isobe, H. and Sato, S. (2021) A case study of stereoisomerism with [6]cyclo[4]helicenylenes. *Chem. Lett.* **50**, 110–112.
- 91) Fujita, S. (1991) Symmetry and Combinatorial Enumeration in Chemistry. Springer-Verlag, Berlin.
- 92) Pólya, G. (1937) Kombinatorische Anzahlbestimmungen für Gruppen, Graphen und chemische Verbindungen. *Acta Math.* **68**, 145–254.
- 93) Ikemoto, K., Kobayashi, R., Sato, S. and Isobe, H. (2017) Entropy-driven ball-in-bowl assembly of fullerene and geodesic phenylene bowl. *Org. Lett.* **19**, 2362–2365.
- 94) Isobe, H., Homma, T. and Nakamura, E. (2007) Energetics of water permeation through fullerene membrane. *Proc. Natl. Acad. Sci. U.S.A.* **104**, 14895–14898.
- 95) Grabowski, Z.R., Rotkiewicz, K. and Rettig, W. (2003) Structural changes accompanying intramolecular electron transfer: Focus on twisted intramolecular charge-transfer states and structures. *Chem. Rev.* **103**, 3899–4031.
- 96) Bren, K.L. (2016) NMR analysis of spin densities. *In Spin States in Biochemistry and Inorganic Chemistry: Influence on Structure and Reactivity* (eds. Swart, M. and Costas, M.). Wiley, New York, pp. 409–434.

(Received May 23, 2022; accepted June 9, 2022)

## Profile

Koki Ikemoto was born in Tokyo in 1987. He graduated from the University of Tokyo in 2009 and received Ph.D. from the University of Tokyo in 2014 under the supervision of Professor Makoto Fujita. He then joined the group of Professor Hiroyuki Isobe at Tohoku University as an Assistant Professor. In 2016, he moved to the University of Tokyo as an Assistant Professor and was promoted to a Lecturer in 2019 and to an Associate Professor in 2022. Representative awards that he received include the Inoue Research Award for Young Scientists (2017) and the Chemical Society of Japan Award for Young Chemists (2020). His current research interests lie in the exploration of synthetic chemistry, material chemistry, and supramolecular chemistry of nanocarbon molecules.



## Profile

Toshiya M. Fukunaga was born in Hyogo in 1997. He majored in organic chemistry at the University of Tokyo and graduated in 2019. He received his M.S. degree in the Department of Chemistry in 2021 under the supervision of Professor Hiroyuki Isobe and was granted a JSPS Research Fellowship for Young Scientists. From 2022, he has been working as an Assistant Professor of the University of Tokyo. His research interests are on the syntheses and properties of nanocarbon molecules.



## Profile

Hiroyuki Isobe was born in Tokyo in 1970. He received his bachelor and master degrees from Tokyo Institute of Technology in 1994 and 1996 with Professors Eiichi Nakamura and Katsumi Kakinuma as actual and formal supervisors, respectively. He entered the Department of Chemistry of the University of Tokyo in 1996, and in the same year, stayed at Princeton University to work on oligosaccharides with Professor Daniel Kahne for three months. He started his academic career as Assistant Professor at the University of Tokyo in 1998 before receiving his Ph.D. degree (1999) and was promoted to Associate Professor in 2004. His early works on amphiphilic/gene-delivery fullerenes were recognized by several awards, including IUPAC Prize for Young Chemists (2000), Young Scientists Research Award in Natural Product Chemistry (2001), Chemical Society of Japan Award for Young Chemists (2004), Osawa Award (2005), Young Scientists Prize from MEXT (2008) and Nozoe Memorial Award for Young Organic Chemists (2009). In 2007, he was appointed as Professor at Department of Chemistry in Tohoku University where he was concurrently assigned as Principal Investigator of AIMR in 2013. He served as a research director of ERATO Isobe Degenerate  $\pi$ -Integration project from 2013 to 2019. In 2016, he moved back to the University of Tokyo. Since 2007, he renovated his lab space seven times, which involved two award-winning labs (Good Design Award, 2014 and 2017). His scientific works on nanocarbon molecules in these labs were recognized by Honorary International Chair Professorship of Taipei Tech (2015), Chemical Society of Japan Award for Creative Work (2016) and Inoue Prize (2017).

